JCI The Journal of Clinical Investigation

A systems biology approach identifies the role of dysregulated PRDM6 in the development of hypertension

Kushan L. Gunawardhana, … , James P. Noonan, Arya Mani

J Clin Invest. 2023. https://doi.org/10.1172/JCI160036.

Research In-Press Preview Cardiology Nephrology

Graphical abstract

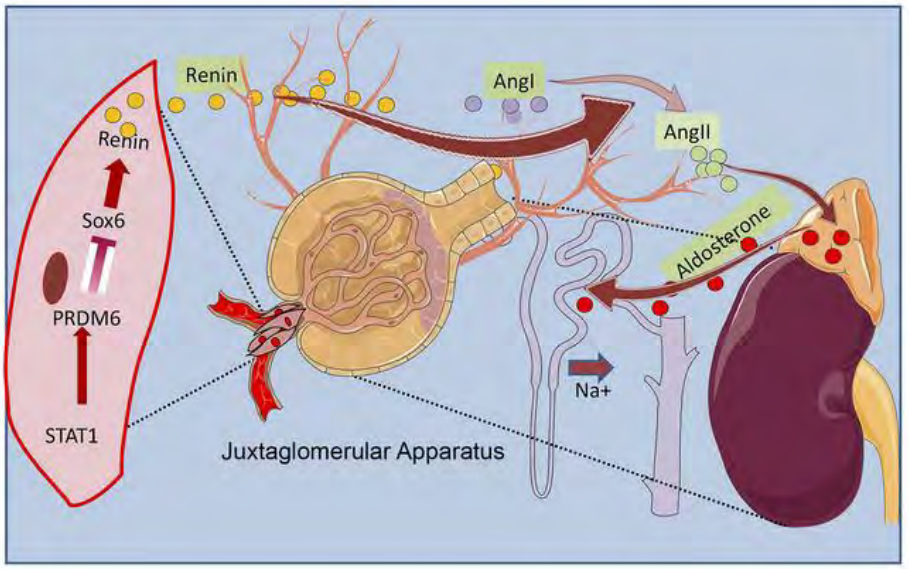

A systems biology approach identifies the role of dysregulated PRDM6 in the development of hypertension

Kushan L. Gunawardhana[1*], Lingjuan Hong[1*], Trojan Rugira[*1], Severin Uebbing[*2], Joanna Kucharczak[3], Sameet Mehta[2], Dineth Karunamuni[2], Brenda Cabera-Mendoza[4], Renato Polimanti[4], James Noonan[1, 2], Arya Mani[1, 2]

[1]Cardiovascular Research Center, Department of Internal Medicine, Yale School of Medicine, New Haven, CT, 06520, USA.

[2]Department of Genetics, Yale School of Medicine, New Haven, CT, 06511

[3] Trinity Hall College, University of Cambridge, Cambridge, UK

[4]Department of Psychiatry, Yale School of Medicine, New Haven, CT, 06511

**Correspondence to:

Arya Mani

Yale Cardiovascular Research Center

300 George Street

New Haven, USA 06511

Email: arya.mani@yale.edu

Tel: 203-7372837

Fax: 203-737-6118.

[*]These authors contributed equally to the manuscript

Abstract

Genetic variants in the third intron of the *PRDM6* gene have been associated with blood pressure traits in multiple genome-wide association studies (GWAS). By combining fine mapping, massively parallel reporter assays, and gene editing we identified the causal variants for hypertension as super-enhancers that drive the expression of *PRDM6* and are partly regulated by STAT1. The heterozygous SMC-specific *Prdm6* knockout mice (*Prdm6fl/+ Sm22Cre*) exhibited a markedly higher number of renin-producing cells in the kidneys at embryonic day 18.5 compared to wild-type littermates and developed salt-induced systemic hypertension that was completely responsive to the renin inhibitor aliskiren. Strikingly, RNA-seq analysis of the mice aorta identified a network of PRDM6-regulated genes that are located in GWAS-associated loci for blood pressure, most notably *Sox6,* which modulates renin-expression in the kidney. Accordingly, the smooth muscle cell-specific disruption of Sox6 in *Prdm6fl/+ Sm22Cre* mice resulted in a dramatic reduction of renin. Fate mapping and histological studies also showed increased numbers of neural crest-derived cells accompanied by increased collagen deposition in the kidneys of *Prdm6fl/+ Wnt1Cre-ZsGreen1Cre* compared to wild-type mice. These findings establish the role of PRDM6 as a regulator of renin-producing cells and an attractive target for the development of antihypertensive drugs.

INTRODUCTION

Systemic vascular hypertension is the largest modifiable risk factor for cardiovascular diseases worldwide(1). Despite intensive investment in developing antihypertensive drugs, about 50% of individuals with hypertension fail to reach the target blood pressure(2), indicating an urgent need for the discovery of novel therapeutic targets.

Blood pressure has a significant heritable component accounting for 30–50% of its variation(3). The identification of genetic variants influencing blood pressure has great potential for the discovery of novel and potent therapeutic targets(4). Genome-wide discovery analyses of blood pressure traits—systolic blood pressure (SBP), diastolic blood pressure (DBP), and pulse pressure (PP) have identified hundreds of loci associated with blood pressure traits(5), but the causal genes remain largely unknown. Several genetic variants in the *PRDM6* locus on Chr5q23.2 have been associated with blood pressure traits by genome-wide association studies in individuals of Western European(6), Finnish(7), and East and South Asian ancestry(8).

PRDM6-encoded protein is a histone modifier that is exclusively expressed in smooth muscle cells (SMCs) in adult life, reaching its highest levels in the SMCs of the aorta and other arteries (9-11) and is, therefore, a great candidate gene for arterial hypertension. During embryonic life, it is also expressed in the neural crest cells(12) , a transient structure that provides inductive signals for organogenesis in diverse tissues, including renal stroma(13). Consequently, we embarked on examining the regulatory landscape of PRDM6*,* to characterize its function and its regulated network and to explore the relationships between the GWAS sequence variations in this gene and blood pressure traits. We used pairwise linkage disequilibrium (LD) measures to identify SNPs that are in LD with the GWAS sentinel SNPs in *PRDM6* gene and used open chromatin and histone marks mapping to refine the locus. To identify the causal variants, we used CRISPR-Cas9 mediated gene editing and multiple parallel reporter assay (MPRA) in HEK293T cells, which are epigenetically well-characterized human embryonic kidney cells that originate from neural crest(14) and abundantly express PRDM6. It is noteworthy that there is a strong overlap and functional conservation of *cis*-eQTLs across different cell types(15-17). Our analysis led to the identification of *PRDM6* super-enhancers that are in LD with lead SNPs in 3rd intron of *PRDM6*in a locus that is densely populated by binding sites for transcription factors, such as STAT1 and CEBPa/b. Interestingly, genetic variants in *STAT1* gene itself have been associated with systolic hypertension (CVDKP. https://cvd.hugeamp.org).

We next focused on exploring the mechanisms by which PRDM6 regulates BP in vivo. We first examined SBP, DBP, and PP in mice with inducible disruption of the *Prdm6* gene in smooth muscle cells (SMC). Observing no difference in any of the BP traits between transgenic mice and wild-type littermates, we considered the developmental role of *Prdm6* in BP regulation. Strikingly, heterozygous SMC-specific knockout mice (*Prdm6fl/+ Sm22Cre*) kidneys exhibited a markedly higher number of renin-producing cells and developed hypertension when fed a high salt diet. The exploration of the disease pathways by bulk RNA sequencing of the aorta led to the identification of a network of Prdm6-regulated genes that have been identified as GWAS loci for hypertension. Among these genes *Sox6* was of particular interest since genetic variants in *Sox6* locus have been associated with blood pressure traits in diverse populations(18) and it has been reported to be a modulator of renin levels in the kidney(19). Further investigations showed that Prdm6 increases renin-producing cells in the embryonic kidney by upregulating Sox6. Taken together, these findings identify PRDM6 as a hub for a network of genes that regulate blood pressure and characterize PRDM6 as a critical regulator for renin-dependent hypertension.

RESULTS

DELINEATION OF THE REGULATORY LANDSCAPE OF *PRDM6* GENE

Several genetic variants in the PRDM6 gene on Chr5q23.2 have been significantly associated with blood pressure traits in individuals of Western European(6), Finnish(7), East and South Asian ancestry(8)(Figure 1A). rs13359291 (pSBP<2.27e-24; pDBP< 2.18e-17; pPP< 48e-17) and rs2287696 (pSBP 4.79e-24; pDBP< 5.36e-18; pPP< 1.42e-16) are associated with all three blood pressure traits, while rs1422279 (pSBP<4.45e-26, pPP<1.57e-30) and rs555625 (pSBP<1.49e-12; pDBP<2.80e-12) are associated with systolic BP (SBP) and one or the other blood pressure traits (T2SKP, https://t2d.hugeamp.org/#). rs13359291 has been identified as a lead SNP by multiple studies. It is an eQTL for *PRDM6* in tibial arteries (P<1.2e-7) and aorta (P<5.7 -4) (GTEx database) (Table1), with net effect sizes of -0.16 and -0.11 respectively. rs2287696, rs1422279, and rs555625 are eQTLs in the aorta (able1). Using LDlink, we carried out pairwise LD analyses using the East Asians genome since the lead SNPs show their strongest effects in this population. The analyses showed that rs13359291, rs2287696 and rs1422279 are in LD with each (R^2>0.65 & D`>0.95) and are located in the 3rd intron of PRDM6 (Figure 1B), in open chromatin regions in the aorta and near histone marks associated with active enhancers (Figure 1C). The lead SNP rs555625 is also located in an open chromatin region of the aorta and is marked by H3K27ac in smooth muscle cells (Figure 1C).

To establish an association between the LD region and *PRDM6* expression we deleted the ~22 kb DNA segment that encompasses all lead SNPs, using CRISPR-Cas9 editing in HEK293T cells (Figure 1D), a cell line of neural crest origin[13] that abundantly expresses PRDM6 (Figure 1E). We screened the sgRNAs (Table S13) based on efficiency score (>60) and self-complementary scores (<1) to increase the gRNA efficacy and eliminated all gRNAs that recognize genomic loci with > 20% sequence similarity to the target sequence to minimize the off-target effect. The off-target effect was further curtailed by characterizing multiple independent deletion lines for downstream analyses. The deletion resulted in a significant reduction in *PRDM6* mRNA expression compared to the wild-type sequence assayed by RT-qPCR, identifying the intronic region as an enhancer locus for PRDM6 (Figure 1F).

MASSIVELY PARALLEL REPORTER ASSAY (MPRA) IDENTIFIES THE CAUSAL SNPS FOR HYPERTENSION

We then carried out an MPRA and investigated the transcriptional regulatory potentials of 336 common variants in the 3rd intron of PRDM6. Based on allelic permutations, we generated 1602 unique MPRA fragments for our experiment. An oligo pool was synthesized based on the sequence information of these unique fragments, such that each fragment contained the genetic variant to be tested, flanked by 68 bp on each side. Additionally, common adaptors were incorporated into the oligos for PCR amplification and restriction enzyme-based cloning as described (20) (Figure 2A). Random barcode oligos were incorporated via emulsion PCR. The resulting inert library was sequenced (MiSeq Paired-End 250 bp) to determine barcodes associated with each fragment. The library consisted of ~1.5 million barcodes distributed among 1602 fragments (Figure 2B), such that >98% of the fragments had at least 12 barcodes associated with differential activity analysis. The competent vector library was constructed by cloning a luciferase reporter gene and minimal promoter (minP) in between fragment and barcode and transfected into HEK293T cells. After 5h incubation, cells were harvested, and DNA and RNA were isolated and sequenced (HiSeq paired-end 150 bp).

The assay revealed that 44 out of 336 SNPs in 37 reporter constructs, either alone or in a combinatorial fashion conferred allele-specific regulation of *PRDM6* (Table 2, Figure 2C-D). Sixteen reporter constructs contained a single, 15 contained 2, and 6 contained 3 SNPs that showed allele-specific activity (Figure 2D, Figure S1A-B). To select candidate SNPs that are causal for blood pressure we prioritized the SNPs that were lead SNPs or were in LD with the lead SNPs for BP traits. There were 5 different LD groups (R^2>0.70) based on the haplotypes generated from lead GWAS SNPs and SNPs discovered by the MPRA (Figure 3A). Strikingly, the lead SNP rs13359291 itself showed significant allele-specific activity as a single SNP in the reporter construct (Table 2). This SNP is in an LD group (LD grp-1) with 13 other SNPs, including the lead SNPs rs1422279 and rs2287696 (Figure 3A). rs368699046 in the LD grp-1 also showed significant allele-specific activity when present as a single SNP in the reporter construct. rs10044090 and rs335158, present in this LD group showed the strongest allele-specific activities in MPRA (Table 2). In LD grp-3 rs459638, rs459678 and rs457807, which were in strong LD with the lead SNP rs555625 showed significant allele-specific activities (Figure 3A, Table

3). rs459638 independently exhibited significant allele specific activities but its effect size was greater when coexpressed with rs459678 and rs182432601(Table 2).

We subsequently performed a colocalization analysis to determine whether the *PRDM6* variants (±750kb) showed shared effects on tissue-specific gene expression and traits related to blood pressure. Our colocalization analysis identified four signals of effects shared between *PRDM6* tissue-specific gene regulation and genetic associations with traits related to blood pressure (Tables S1-S12, please see excel sheets). The variants identified were all in high LD (R^2>0.9) with the *PRDM6* validated experimentally (Supplemental Figure S2). Specifically, rs1422279 showed multiple colocalization signals: i) of *PRDM6* aorta-artery gene regulation with pulse pressure (LD proxy: rs1624823, PP_{H4} =0.952) and systolic blood pressure (LD proxy: rs1624822, PP_{H4} =0.948); ii) between *PRDM6* tibial-artery gene regulation and pulse pressure (LD proxy: rs1624823, PP_{H4} =0.921). Rs13359291 showed colocalization evidence between *PRDM6* tibial-artery gene regulation and systolic blood pressure (LD proxy: rs10052206, PP_{H4} =0.656).

In summary, the MPRA identified in total 7 SNPs (Table 3) in LD grp-1 and LD grp-3 as functional SNPs. The finding suggested the existence of clusters of enhancers in the intron 3 of *PRDM6* gene, comprising an array of sequence elements that work together to regulate blood pressure. According to ChIP-Seq data from multiple tissue types available from ENCODE and Roadmap Projects(21) the super-enhancer locus spans a DNA sequence that is densely occupied by transcription factors (TF), most notably STAT1 (Supplementary Figure S3). We subsequently confirmed the allele-specific effects of these SNPs in the endogenous genomic context by CRISPR-based genome editing in HEK293T cells, verified their deletion by Sanger sequencing, and assayed for *PRDM6* transcripts using RT-qPCR. We first deleted rs13359291, since it is associated with all BP traits, is a lead SNP in multiple GWASes, is an eQTL for *PRDM6* in the tibial artery and aorta (Figure 3B) and is located in an open chromatin region of the aorta (Figure 3C), albeit being only partially conserved (Figure 3C, zoomed). sgRNAs were designed to delete the 52 bp region encompassing rs13359291 and independent deletion lines were verified as previously described (Table S13). PROMO tool based in silico motif finder, predicts rs13359291 to be a putative binding site for CEBP beta and alpha (Figure 4A, Table 4), which are known regulators of renin-angiotensin-aldosterone system(22, 23)**.** Using RT-qPCR we found a significant downregulation in *PRDM6* mRNA expression in the CRISPR-Cas9-deleted compared to

wild-type cells (Figure 4B). We then deleted rs457807 which similarly showed allele-specific activity in MPRA, and together with the lead SNP rs555625 is in LD grp-3. Interestingly, we observed a significant change in *PRDM6* expression with the deletion of this SNP as well (Figure 4C).

Taken together, these findings solidified the presence of a super-enhancer in the intron 3. ChIP-Seq analysis according to ENCODE has identified a cluster of binding sites for STAT1 in this locus. Interestingly, a splice region variant in *STAT1* (rs2066804) has been associated with reduced blood pressure (CVDKP. https://cvd.hugeamp.org). Consequently, we focused on SNPs that showed differential expression and are located within the STAT1 binding sites. We first deleted a ~2 kb STAT1 binding region in the LD grp-1, encompassing rs368699046 (Table 2) and is in LD with the 2 lead SNPs rs13359291 and rs2287696 (Table 3). This deletion significantly reduced the *PRDM6* expression in comparison to the wild-type control (Figure 4D). Next, we deleted rs145044129, which also showed allele-specific activity in MPRA and is flanked by a STAT1 binding region on the 3rd intron of *PRDM6*. CRISPR-Cas9 mediated deletion of rs145044129 along with STAT1 binding locus reduced *PRDM6* expression significantly as well(Figure 3F). Since interferon-gamma (IFNγ) stimulates pSTAT1-dependent gene activation(24), we proceeded with IFNγ (100ng/mL, 4 hours) stimulation of HEK293T cells with and without CRISPR deletions encompassing STAT1 binding regions. The results showed that the expression of *PRDM6* is increased upon stimulation with IFNγ in wild-type HEK293T cells, while no significant changes in both CRISPR deleted lines were noted (Figure 4D), highlighting the role of STAT1 as a transcription factor regulating PRDM6 transcription. Taken together, our data suggest the PRDM6 expression is regulated by a super-enhancer that is located in intron 3 and contains binding sites for multiple TFs, including STAT1.

THE HETEROZYGOUS SMC-SPECIFIC PRDM6 KNOCKOUT MICE DEVELOP HYPERTENSION IN RESPONSE TO A HIGH-SALT DIET

We then proceeded to examine PRDM6-regulated disease pathways in vivo by generating inducible conditional SMC *Prdm6* knockout mice. We intercrossed *Prdm6fl/fl* female mice on C57BL/6J background with SMMHC-CreER^{T2} male mice, which were on the same background and express CreER^{T2} under the control of the mouse smooth muscle myosin heavy polypeptide 11(*Myh11*) promoter/enhancer regions on the Y chromosome. All mice were fed a chow diet and

received tamoxifen (100µg) injections for 3 consecutive days (P1-P3). The 15-20 months old mice underwent invasive telemetry-based blood pressure monitoring and were introduced to a high salt diet (8% NaCl – Research Diets, D05011703) on the 6th day of blood pressure monitoring. Surprisingly, no change in systolic or diastolic blood pressure was noted in transgenic mice compared to their wild-type littermates (Figure S4A). We hypothesized that Prdm6 developmentally regulates blood pressure and decided to examine BP in heterozygous SMC-specific *Prdm6* knockout mice since homozygous mice die on ~P1-2(12). Thus, 15-20 weeks old heterozygous (*Prdm6fl/+ Sm22Cre*) mice fed with a chow diet were introduced to a high salt diet and underwent telemetry-based BP measurements. Both female and male, wild-type and transgenic mice showed a rise in SBP and DBP when placed on a high salt diet, but heterozygous KO mice showed a much greater rise in SBP, DBP, and PP compared to wild-type littermates (Figure 5A-C), most dramatically during the resting phase (Figure 5D-F), when paradoxically the mutant mice were more active compared to their littermate controls (Figure S4B).

PRDM6 CONTROLS BLOOD PRESSURE VARIATION BY RESTRAINING RENIN PRODUCING CELLS

To investigate the molecular mechanisms by which Prdm6 controls BP we embarked on performing an RNA-Seq of the aortic tissues of homozygous SMC-specific knockout mice (*Prdm6fl/fl Sm22Cre*) and their littermate controls for RNA-Seq at P0.5. The analysis showed 1118 differentially expressed transcripts in *Prdm6fl/fl Sm22Cre* vs. wild-type mice (P-value < 0.05). 349 transcripts were upregulated while 769 were downregulated in *Prdm6fl/fl Sm22Cre* vs. wild-type mice aortas (Figure 6A). Strikingly, 43 genes are localized at the peak GWAS loci for BP traits (Figure 6B). A significant number of these genes were associated with multiple BP traits (Figure 6C). The gene-set enrichment analysis using PartekFlow software identified many blood pressure-related processes that were enriched with both up and down-regulated genes(Figure 6D-E). Similarly, the analysis identified a number of pathways related to BP regulation, most notably the renin-angiotensin-aldosterone system (RAAS) (Figure S5).

Renin is secreted from the juxtaglomerular (JG) cells of the kidney in response to hypotension, adrenergic stimulation, or low salt. These cells are precursors for arteriolar smooth muscle, mesangial cells, and interstitial pericytes (25) which are mainly within the walls of the afferent arterioles in macula densa (Figure 7A). *Prdm6fl/+ Sm22Cre* mutants have enlarged kidneys

despite equal body weights (Figure 7B). Consistent with the RNA-Seq analyses results, we observed higher total renin mRNA and protein levels in the kidneys and also observed increased aldosterone synthase mRNA levels in the adrenal glands of adult *Prdm6fl/+ Sm22Cre* mice vs. wild-type littermates (Figure 7C-D). Accordingly, the fraction of sodium excretion showed a trend towards a reduction in *Prdm6fl/+ Sm22Cre* vs. WT mice fed with a high salt diet(Figure 7E). These findings indicated increased RAAS activation in *Prdm6fl/+ Sm22Cre* mice compared to wild-type littermates. During embryogenesis, renin is expressed initially in the smooth muscle cells of larger intrarenal arteries but in adult mice, it is restricted to the terminal part of the preglomerular arterioles and coexpressed with α-smooth muscle actin (αSMA)(26). Strikingly, the immunofluorescence staining of *Prdm6fl/+ Sm22Cre* and *Prdm6fl/fl Sm22Cre* mice kidneys for renin on E18.5 showed an increased number of renin-expressing cells compared to their corresponding wild-type littermates (Figure 7F, G). Interestingly, we found no change in renin expression intensity per cell among the genotypes (Figure 6H), suggesting that Prdm6 does not control renin expression but it regulates the number of renin-producing cells. Renin is normally suppressed in normal mice on a high salt diet or with essential hypertension. To establish the causal role of renin in *Prdm6fl/+ Sm22Cre* mice hypertension we fed them a high salt diet and simultaneously treated them with the renin inhibitor aliskiren by daily oral gavage (50mg/kg). The blood pressures were measured for a total of 11 days on a high salt diet by tail-cuff method. All mice had a normal growth curve (Figure S6) and did not exhibit any apparent sign of distress during the entire experimental period. Although, it is plausible that the continuation of high-concentration salt could have resulted in adverse outcomes such as end-organ damage. As expected, the aliskiren was able to fully normalize the elevated blood pressure in *Prdm6fl/+ Sm22Cre* mice but had no effect on the systolic or diastolic blood pressure of wild-type mice(Figure 7I). This finding supports the causal role of renin as a mediator for PRDM6 regulation of blood pressure.

PRDM6 CONTROLS RENIN-PRODUCING CELLS BY TRANSCRIPTIONAL REGULATION OF *SOX6*

Sox6 was one of the upregulated genes in RNA-Seq of *Prdm6fl/fl Sm22Cre* mice aorta (Figure 8A). Sox6 is highly expressed in juxtaglomerular cells, is upregulated by a high salt diet, and triggers the recruitment and differentiation of renal mesenchymal stem cells to renin-producing cells (19). Strikingly, the *Sox6* gene locus has been associated with SBP, DBP, and PP(27).

The immunofluorescent staining of heterozygous and homozygous *Prdm6* knockout mice kidneys for *Sox6* showed increased numbers of Sox6 positive cells compared to the wild-type littermates (Figure 8B). Accordingly, 22 kb CRISPR deletion of the *PRDM6* enhancer region resulted in a dramatic increase of *Sox6* expression level in HEK293T cells (Figure 8C). Based on the ENCODE dataset (*doi:10.17989/ENCSR892QHR*) PRDM6 binds to several regulatory regions of the *Sox6* gene in HEK293T cells (Figure 8D). Taken together, our findings indicate that Prdm6 regulation of renin-expressing cells is attained by transcriptional regulation of the *Sox6* gene. To support our finding we disrupted *Sox6* in *Prdm6* KO mice by intercrossing *Sox6fl/fl* and *Prdm6fl/+* and *Sm22-Cre* mice. While *Sox6fl/fl Prdm6fl/fl Sm22-Cre* were embryonically lethal, we were able to show a markedly reduced number of renin-producing cells in their kidneys compared to control (*Sox6fl/fl Sm22-Cre* mice on E18.5 (Figure 8E). Taken together these findings indicated that Prdm6 developmentally regulates renin-producing cells by inhibiting *Sox6* expression.

The mesodermal origin of the renin-producing cells

Sox genes play key roles in fate specification, cellular differentiation, and neural crest development during embryonic life (28). PR/SET(PRDM) family of proteins are also highly expressed in the neural crest cells (29)and participate in transcriptional regulation via chromatin remodeling and are involved in temporal and spatial regulation of gene regulatory networks necessary for proper neural crest development in mice (30) and zebrafish (31) or are downstream targets of the transcription factors that regulate the formation of neural crest (32). Prdm6 is expressed in cardiac NCCs and regulates SMC specification (12). Given that renin-secreting juxtaglomerular cells are of smooth muscle cell lineage(26), we used fate mapping to examine if renin-producing SMCs in *Prdm6fl/fl Sm22Cre* mice are derived from NCCs. To this end, we intercrossed *Prdm6fl/fl Wnt1-Cre* and *Zs1Greenfl/fl* mice, which are both on C57BL/6J background, and examined the presence of Zs1Green in the kidneys at E17.5. There were considerably greater numbers of Zs1Green positive cells in the kidneys of *Prdm6fl/fl Wnt1Cre,* which localized mainly adjacent to the vessel walls (Figure 9A). The renin level was not significantly different and did not colocalize with Zs1Green in *Prdm6fl/fl Wnt1Cre* or wild-type mice (Figure 9B). Surprisingly, there were reduced levels of Sox6 (Figure 9C) in *Prdm6fl/fl Wnt1Cre* vs. wild-type mice. Only a small fraction of the Sox6 colocalized with Zs1Green. To establish the

role of mesodermal PRDM6 in renal Sox6 expression we proceeded to fate map SMCs in *Prdm6fl/fl Sm22-Cre* mice by crossbreeding them with *Zs1Greenfl/fl* mice. As shown earlier, we noted increased Zs1Green cells that expressed Sox6 in *Prdm6fl/+ Sm22-Cre Zs1Green* compared to *Prdm6+/+ Sm22-Cre Zs1Green* (WT) mice (Figure 10A), indicating that loss of PRDM6 in SMCs increases SMCs of mesodermal lineage, which expresses Sox6. Taken together these findings show that loss of PRDM6 in the mesodermal but not NCC-derived cells results in increased Sox6 levels in the kidney.

Since NCCs can differentiate into myofibroblasts (33) we examined if the transformation of migrating NCCs into myofibroblasts and deposition of collagen contributes to the larger size kidney in *Prdm6fl/fl Wnt1-Cre* vs. wild-type littermates. There was modest colocalization of PDGFRβ and Zs1Green positive cells in *Prdm6fl/fl Wnt1-Cre* mice, providing indirect evidence for their myofibroblast identity(Figure 10B). Accordingly, there was increased Sirius red staining as evidence for increased collagen deposition in the interstitium of 12 weeks *Prdm6fl/fl SM22-Cre* (heterozygous) mice kidneys compared to wild-type mice(Figure 10C). Interestingly, STAT1, the upstream transcriptional regulator of PRDM6 expression has been shown to be protective against renal interstitial fibrosis after ischemia-reperfusion injury (34). If the interstitial collagen also contributed to the elevated BP as shown in systemic sclerosis (35) could not be determined. The large size of the kidneys in *Prdm6fl/fl SM22-Cre* mice was also contributed by larger glomeruli and renal tubules, which were associated with lower plasma creatinine levels compared to wild-type littermates (Figure 10D, E). Improved GFR may reflect increased hydrostatic pressure due to the higher systemic blood pressure.

Taken together, our study establishes the role of PRDM6 as a hub for a network of genes that regulate blood pressure in part by controlling the abundance of renin-producing cells.

DISCUSSION

In this study, we use a systems biology approach to establish a link between GWAS variants at the *PRDM6* gene locus, the altered expression of *PRDM6,* and the development of systolic and diastolic hypertension. By combining LD analysis, a high throughput reporter assay, and CRISPR-Cas9 mediated gene editing we first mapped the regulatory landscape of the *PRDM6* gene and identified a super-enhancer locus that is a binding site for numerous

transcription factors, most notably STAT1. Interestingly, genetic variants in STAT1 locus and hypertension loci that are enriched for STAT1 binding sites have been associated with hypertension (36). We then demonstrated a link between reduced PRDM6 transcript levels and the development of hypertension *in vivo*. Strikingly, hypertension developed only when PRDM6 was disrupted embryonically, indicating the developmental role of PRDM6 in BP regulation.
The delineation of the disease pathways led to the discovery of PRDM6 as an embryonic regulator of renin-expressing cells in the kidney. Renin is a component of RAAS that plays a central role in the regulation of blood pressure, and electrolyte homeostasis(37). In the developing kidney, the expression of renin is detectable at E*14.5* in a subset of SMCs in the arcuate arteries(26). Later, most renin-producing cells differentiate into arteriolar smooth muscle, mesangial cells, and interstitial pericytes, and consequently, renin expression shifts from proximal to distal parts of the tree and t remains restricted to a small segment in renal afferent arteriole known as juxtaglomerular (JG) cells (25, 38). The differentiated cells retain the memory to re-express renin to maintain homeostasis under physiological (25) and pathological conditions (39)by mechanisms that are not fully understood. PRDM6 is a histone modifier that plays a critical role in VSMC specification (12). Our findings suggest that loss of PRDM6 impairs Sox6-dependent differentiation of renin-producing cells in mesodermal-derived SMCs, resulting in an increased number of renin-producing cells in the kidney. The potential role of PRDM6 in other tissues in the regulation of BP traits was not examined in our study.

The RNA-Seq analysis of the aorta suggested that PRDM6 functions as a multifaceted protein that regulates the expression of a number of genes located in GWAS-loci for BP and thus, functions as a hub for a network of blood pressure-regulating proteins. Among PRDM6-regulated gene networks, the *Sox6* gene was of particular interest as its encoded protein regulates the recruitment and differentiation of renal MSCs to renin-producing cells (19). Accordingly, our transcriptomic analysis followed by in vivo genetic rescue studies established the causal role of Sox6 in mediating PRDM6-regulation of renin-producing cells.

Fate mapping studies have suggested the involvement of lumbosacral NC crest (NC) cells in kidney organogenesis(13) and their contribution to renal interstitial fibroblasts (33). Others have proposed that interstitial fibroblasts are derived from mesenchymal FoxD1-positive progenitor cells(40) or *NKD2*-positive pericytes and myofibroblasts(41). We have previously shown that PRDM6 is expressed in both mesodermal and neural crest cell-derived SMCs(12). By using

fate-mapping we show here that loss of PRDM6 in Wnt1-positive NCCs does not alter renin expression but may result in a modest increase in PDGFR-positive NCC-derived cells, and increased collagen deposition in the kidney. Whether renal interstitial collagen deposition contributes to increased blood pressure (35) is not known. It is noteworthy that STAT1 has been shown to be protective against renal fibrosis during renal injury (34). In conclusion, our study establishes the role of PRDM6- as a master regulator of blood pressure and as an attractive target for the treatment of hypertension.

Methods

Generation of SM22-Cre knockout mice

All animal procedures were carried out as per approved by a protocol of the Yale University Institutional Animal Care and Use Committee (IACUC). The day of plug detection was considered E0.5. Prdm6-flox mice were kindly provided by Dr. Jürgen Ruland's laboratory in Germany and were intercrossed to generate homozygous Prdm6 floxed mice (*Prdm6fl/fl*). Homozygous Prdm6 floxed mice (*Prdm6fl/fl*) were viable, fertile, and indistinguishable from control littermates. Homozygous mice *Prdm6fl/fl* were intercrossed with SM22-Cre transgenic mice that express high levels of Cre recombinase in smooth muscle cells. While homozygous progenies *Prdm6fl/fl SM22-Cre* died shortly after the birth from a patent ductus arteriosus *Prdm6fl/+ SM22-Cre* mice were perfectly healthy and developed high blood pressure only after being placed on a high salt diet. *Sox6fl/fl* transgenic mice were the generous gift of Dr. Monique Lefebvre at the Cleveland Clinic).

Invasive Arterial Pressure Monitoring in Mice

Eight weeks old male Prdm6fl/+ SM22-Cr mice and the wild-type littermates were anesthetized and placed on heating pad to maintain their temperature at 37.0 – 38.0°C. The tip of the radiotelemetric device TA11PA-C10 (Data Sciences Int., United States) was implanted into the common carotid artery toward the heart attached to SI TA11PA-C10 transmitter placed in a pouch underneath the skin along the mouse flank. Mice were fed an 8% salt diet. The rationale for use of a high salt diet was its higher success rate in causing hypertension in heterozygous loss of function mice in prior studies and the fact that other models such as DOCA salt and AngII would have caused RAAS activation downstream from renin. The recordings of the heart rate and beat-by-beat arterial blood pressure started 7 days after surgery for acclimation. Data were analyzed using the Dataquest ART version 2.1 (Data Sciences International).

Tail Cuff Blood Pressure Measurement

Repeat blood pressure measurements using renin inhibitor aliskiren were determined in conscious *Prdm6fl/+ SM22-Cr* mice and the wild-type littermates using a non-invasive computerized automated tail-cuff system (Vistech BP-2000 Blood Pressure Analysis System) and after 15 minutes daily training for five consecutive days. All mice were fed a high salt diet

and either received aliskiren oral gavage (50mg/kg) or water; an average of three 10-cycle was used for blood pressure calculation using BP-2000 software.

Mouse embryo and tissue preparation and immunohistochemistry

Mouse embryos were collected and incubated for 15–20 min in PBS containing 4% PFA (Catalog# sc-281692) at 4°C and after rinsing twice in ice-cold PBS incubated for 24 h in 30% sucrose/PBS at 4°C, followed by embedding in Tissue-Tek O.C.T. compound (Catalog# 4583) in plastic molds on dry-ice until frozen and stored at -80°C. The tissue was sectioned into 5µm -10 µm slices in a cryostat and dried on Superfrost Plus slides (Catalog# 22-037-246) for 12 to 16h at RT.

Immunofluorescence

5µm -10 µm frozen sections were stained using immunofluorescent antibodies. All primary and secondary antibodies were diluted at 1:300. In most cases only validated and previously published antibodies were used. Otherwise, no primaries, knockout mice as well as tissues not expressing the proteins were used as controls. Fluorescence images were obtained by Zeiss 4 laser Confocal microscope or Lecia sp8 and the intensities were measured using the same laser settings for each set of antibodies tested and quantified with Image J and adjusted for the area. The following antibodies for immunostaining were used: anti-SOX6 antibody (Novus, Cat #NBP1-85811), anti-SMA antibody (Abcam, Cat #ab220179), and anti-renin antibody (Novus, Cat #NBP1-31559).

IF image analyses for co-localization and intensity measurement were conducted using ImageJ and CellProfiler tools.

Collagen staining

5µm -10 µm fresh sections were stained using Vitroview Picro-Sirius Red Stain kit (VB-3017) as described in the protocol. The sections are covered with Weigert's Hematoxylin solution for 8 minutes, followed by Picro-Sirius Red stain for 60 minutes. Then slides were washed with acidified water, water, ethanol (95% and 100%) and finally xylene. Subsequently slides were covered with a coverslip along with Permount. Slides were images under the Nikon 80i microscope system.

Bulk RNA Sequencing

The RNA was isolated using Trizol, reverse-transcribed to cDNA, fragmented and ligated with sequencing adaptors with a 4 µl used as input for RNA library preparation. Sequencing libraries were generated using v2 - Pico Input Mammalian kit(Takara, 634413) and quality controls were done with the Fragment Analyzer high sense small fragment kit (Agilent Technologies, sizing range 50 bp-1000 bp). Samples were pooled and loaded on the NextSeq. 500 (Illumina) with a loading concentration of 1.2 pM at the YCGA. The reads were trimmed for quality and length with a minimal base quality of Q30, and a minimum length of 45. The reads were aligned to the mouse UCSC reference genome mm10 (42, 43)using TopHat2(44). The alignment data was converted to per-gene counts using cufflinks(45), and further analyzed using cuffdiff and R and visualized using R as described elsewhere (http://www.r-project.org/index.html).

CRISPR-Cas9 deletion line generation

Vector construction, plasmid transformation & clonal line recovery was carried out as explained (46). In brief, sgRNA sequences designed using CHOPCHOP (https://chopchop.cbu.uib.no/) were cloned into the pSpCas9(BB)-2A-GFP vector as outlined. Then plasmids were transfected into HEK293T cells, obtained from ATCC and allowed to recover. %GFP expression was used to determine transfection efficacy. Clonal lines were recovered with serial dilutions as described in the protocol. The deletion lines were verified using PCR and sequencing. Multiple lines were characterized to determine consensus phenotype and proceeded with one of the lines.

Massively parallel reporter assay and data analysis

We identified 336 common genetic variants located on the 3rd intron (chr5:123,099,000-123,156,999, GRCh38) of the *PRDM6* gene. For each of these common variants, an oligo was designed such that the variant was in the center of a 137 bp oligo sequence. Some MPRA fragments contained additional genetic variants that were near to the one that was in the middle. For such fragments, all possible allele combinations were planned to be tested. This study plan resulted in 1602 unique MPRA fragments. Oligo pool generation, library construction, library

transfection, sequencing and data analyses were carried out as explained elsewhere (20). In brief, oligos were tagged with random, 16 bp barcode tags using emulsion PCR. This inert library was sequenced (Illumina MiSeq 2x 250 bp) to establish oligo–barcode connections. A luciferase reporter gene and a minimal promoter were cloned in between oligo and tag, such that the barcode was incorporated into the 3' end of the reporter gene. This competent library was then transfected into HEK293T cells using a Polyplus transfection kit, and the 3' end of the reporter gene was sequenced as plasmid DNA (pDNA) and mRNA (complementary DNA, cDNA) libraries (Illumina HiSeq 2x 150 bp). Read counts were summarized by barcode tag, normalized by library size, and $\log_2$ transformed. As small data values show a Poisson-like distribution, we determined a lower-end cutoff by plotting each library's distribution and removing normalized values below 0.5. The cDNA values were normalized by their corresponding pDNA values to produce the "activity" of each barcode tag. Barcode tags were then ascribed to the fragment they originated from and fragments with fewer than 12 barcode tags were excluded from downstream analyses. We identified variants that affected MPRA activity by performing a student's *t-test* between the activity of barcode tags of any fragment that contained a variant, relative to those of the wild-type reference fragment.

Western blot and quantification

WB was done using standard procedures and the membrane was developed by Supersignal West Pico (Catalog#34580) and Supersignal West Femto (Catalog#34096). The WB was quantified by ImageJ as described (47). The anti-renin antibody (Novus, Cat #NBP1-31559) and anti-GAPDH (Abcam, Cat#ab9485) were used.

RNA extraction and RT-qPCR

RNA extraction and RT-qPCR were performed as described (48), with minor modifications. Tissues/cells were collected and frozen. Total RNA was isolated using RNeasy Plus Mini kit (QIAGEN, Cat#74134) and cDNA was synthesized using Superscript II (Invitrogen). The reverse transcription (RT) product was amplified with SsoFast qPCR Supermix (Bio-Rad) in a Bio-Rad CFX96 Real-Time PCR System using pairs of gene-specific primers. Human-*ACTB*-Forward: CACTCTTCCAGCCTTCCTTC, Human-*ACTB*-Reverse:

GATGTCCACGTCACACTTCA, Human-*PRDM6*-Forward: GGTGGGGAACCTAG-TAAGTCG, Human-*PRDM6*-Reverse: ACCGTTGAAGGGACATTTAAGTT, Human-*SOX6*-Forward: CTGCCTCTGCACCCCATAATG, Human-*SOX6*-Reverse: TTGCTGA-GATGACAGAACGCT, MOUSE-*Actb*-Forward: TGTGACGTTGACATCCGTAAAG, MOUSE-*Actb*-Reverse: GCAGTAATCTCCTTCTGCATCC, MOUSE-*Ren*-Forward: GTG-GACATGACCAGGCTCAGTG, MOUSE-*Ren*-Reverse: CACCCAGAGGTTGGCTGAACC, MOUSE-*Aldos*-Forward: TGGCTGAAGATGATACAGATCCT, MOUSE-*Aldos*-Reverse: CACTGTGCCTGAAAATGGGC.

Neural crest cells fate mapping

.

Wnt1-Cre2 mice, stock number 022501(*B6.Cg-E2f1Tg(Wnt1-cre)2Sor/J*) and *ZsGreen1* (*Rosa-CAG-LSL-ZsGreen1-WPRE*, Jax 007906) were purchased from The Jackson Laboratory. For lineage tracing, *Prdm6fl/fl* mice were intercrossed with *Zs1Greenfl/fl* mice. To knock out *Prdm6* in *Wnt1* positive neural crest cells the *Prdm6fl/+ Zs1Greenfl/fl* mice were further inter-crossed with *Prdm6fl/+ Wnt1-Cre2* mice. All studies in animals were conducted in accordance with the National Institutes of Health Guidelines for the Care and Use of Laboratory Animals.

Mouse embryo and tissue preparation and immunohistochemistry

Mouse embryos and tissues were collected and rinsed in ice-cold DPBS and fixed by in-cubation for 15–20 minutes in PBS containing 4% PFA (Catalog# sc-281692) at 4°C. They were rinsed twice in ice-cold PBS and incubated for 24 hours in 30% sucrose/PBS at 4°C, followed by Tissue-Tek O.C.T. compound (Catalog# 4583) in plastic molds, and allowed to freeze on dry-ice and stored at -80°C. The tissue submerged in O.C.T. compound was sectioned into on 5µm -10 µm slices in a cryostat and dried on Superfrost Plus slides (Catalog# 22-037-246) 12 to 16hrs at room temperature (RT).

Locomotor activity measurement

6-8 weeks old mice were habituated for two weeks and individually housed in cages with wheel-running activity continuously recorded for two weeks using the Clocklab6 tool

(www.actimetrics.com). Locomotor activity was monitored at 5-min binned intervals and activity data are displayed as actograms, as described (49).

Colocalization analysis

Colocalization analysis to determine whether the *PRDM6* variants (±750kb) showed shared effects on tissue-specific gene expression and traits related to blood pressure. This analysis was performed with the *coloc* R package (PMID: 24830394) using aorta, coronary, and tibial artery tissues with gene expression data from GTEx Release V7 and GWAS summary statistics related to high blood pressure (n=458,554; PMID: 30940143), systolic blood pressure, diastolic blood pressure, and pulse pressure. from European-descent individuals (n= 757,601; PMID: 30224653). Evidence of colocalization between GWAS and eQTL signals was considered when the posterior probability of colocalization (PP_{H4}) > 0.5. Linkage disequilibrium (LD) of the variants with evidence of colocalization with the *PRDM6* SNPs (i.e., rs13359291, rs1422279, rs555625, and rs2287696) prioritized in the previous experiments were calculated using LDlink (PMID: 26139635) and considering 1,000 Genomes Project European-descent populations as reference panel.

Statistical analyses

In vivo studies included a minimum of five mice in each group. In vitro studies were carried out in more than three independent experiments. The comparison between different groups was done by a 2-tailed unpaired t-test. The normalcy was tested by the Kolmogorov-Smirnov test. F-statistic was calculated to determine if variances were different between samples and the p-values were then Welch corrected. The comparisons between multiple groups were done by one-way ANOVA. Mann-Whitney test was conducted for non-normally distributed data. Fisher's exact test was carried out for the continuous variables. The preparation of graphs and all statistical analyses, including two-tailed Student's *t*-tests, and two-way ANOVA (SigmaPlot). $P < 0.05$ was considered significant. Data are presented as means ± s.e.m. Fluorescence images were evaluated using Image J software (National Institutes of Health).

Study approval

The present studies in animals and/or humans were reviewed and approved by the Institutional Animal Care & Use Committee (IACUC) at Yale, New Haven, CT.

Code and Data Availability

All differential gene expression analyses from bulk and scRNA-Seq and their associated metrics have been deposited in NCBI's Gene Expression Omnibus (GSE195590)

Author contributions

Kushan L. Gunawardhana conducted most experiments, acquired and analyzed data
Lingjuan Hong conducted some of the experiments, acquired and analyzed data
Trojan Rugira did the mice breeding, performed all the revised experiments
Severin Uebbing analyzed Massively parallel reporter assay data
Joanna Kucharczak assisted Kushan L. Gunawardhana in experiments
Sameet Mehta analyzed GWAS data
Brenda Cabera-Mendoza did the colocalization analysis
Renato Polimanti supervised the colocalization analysis
Dineth Karunamuni assisted Kushan L. Gunawardhana in experiments
James Noonan supervised the analysis of Massively parallel reporter assay
Arya Mani designed and supervised the research studies and wrote the manuscript.

Acknowledgments

We thank Dr. Monique Lefebvre (Cleveland Clinic) for generously providing the *Sox6fl/fl* transgenic mice.

This work was supported by grants from the National Institute of Health # RHL135767A to A.M., The authors acknowledge the support of The George M. O'Brien Kidney Center at Yale led by Dr. Preisig for their assistance in invasive blood pressure monitoring.

Conflict of interest statement: The authors have declared that no conflict of interest exists.

Literature Cited

1. O'Seaghdha CM, Perkovic V, Lam TH, McGinn S, Barzi F, Gu DF, et al. Blood pressure is a major risk factor for renal death: an analysis of 560 352 participants from the Asia-Pacific region. *Hypertension.* 2009;54(3):509-15.
2. Buhnerkempe MG, Prakash V, Botchway A, Adekola B, Cohen JB, Rahman M, et al. Adverse Health Outcomes Associated With Refractory and Treatment-Resistant Hypertension in the Chronic Renal Insufficiency Cohort. *Hypertension.* 2021;77(1):72-81.
3. Miall WE, and Oldham PD. The hereditary factor in arterial blood-pressure. *Br Med J.* 1963;1(5323):75-80.
4. Nelson MR, Tipney H, Painter JL, Shen J, Nicoletti P, Shen Y, et al. The support of human genetic evidence for approved drug indications. *Nat Genet.* 2015;47(8):856-60.
5. Evangelou E, Warren HR, Mosen-Ansorena D, Mifsud B, Pazoki R, Gao H, et al. Genetic analysis of over 1 million people identifies 535 new loci associated with blood pressure traits. *Nat Genet.* 2018;50(10):1412-25.
6. Wain LV, Vaez A, Jansen R, Joehanes R, van der Most PJ, Erzurumluoglu AM, et al. Novel Blood Pressure Locus and Gene Discovery Using Genome-Wide Association Study and Expression Data Sets From Blood and the Kidney. *Hypertension.* 2017.
7. Gaal EI, Salo P, Kristiansson K, Rehnstrom K, Kettunen J, Sarin AP, et al. Intracranial aneurysm risk locus 5q23.2 is associated with elevated systolic blood pressure. *PLoS Genet.* 2012;8(3):e1002563.
8. Kato N, Loh M, Takeuchi F, Verweij N, Wang X, Zhang W, et al. Trans-ancestry genome-wide association study identifies 12 genetic loci influencing blood pressure and implicates a role for DNA methylation. *Nat Genet.* 2015;47(11):1282-93.
9. Li N, Subrahmanyan L, Smith E, Yu X, Zaidi S, Choi M, et al. Mutations in the Histone Modifier PRDM6 Are Associated with Isolated Nonsyndromic Patent Ductus Arteriosus. *Am J Hum Genet.* 2016;99(4):1000.
10. Davis CA, Haberland M, Arnold MA, Sutherland LB, McDonald OG, Richardson JA, et al. PRISM/PRDM6, a transcriptional repressor that promotes the proliferative gene program in smooth muscle cells. *Mol Cell Biol.* 2006;26(7):2626-36.
11. Wu Y, Ferguson JE, 3rd, Wang H, Kelley R, Ren R, McDonough H, et al. PRDM6 is enriched in vascular precursors during development and inhibits endothelial cell proliferation, survival, and differentiation. *J Mol Cell Cardiol.* 2008;44(1):47-58.
12. Hong L, Li N, Gasque V, Mehta S, Ye L, Wu Y, et al. Prdm6 controls heart development by regulating neural crest cell differentiation and migration. *JCI Insight.* 2022.
13. Itaranta P, Viiri K, Kaartinen V, and Vainio S. Lumbo-sacral neural crest derivatives fate mapped with the aid of Wnt-1 promoter integrate but are not essential to kidney development. *Differentiation.* 2009;77(2):199-208.
14. Lin YC, Boone M, Meuris L, Lemmens I, Van Roy N, Soete A, et al. Genome dynamics of the human embryonic kidney 293 lineage in response to cell biology manipulations. *Nat Commun.* 2014;5:4767.
15. Ben-David E, Boocock J, Guo L, Zdraljevic S, Bloom JS, and Kruglyak L. Whole-organism eQTL mapping at cellular resolution with single-cell sequencing. *Elife.* 2021;10.

16. Smith EN, and Kruglyak L. Gene-environment interaction in yeast gene expression. *PLoS Biol.* 2008;6(4):e83.
17. Consortium GT. The GTEx Consortium atlas of genetic regulatory effects across human tissues. *Science.* 2020;369(6509):1318-30.
18. Johnson T, Gaunt TR, Newhouse SJ, Padmanabhan S, Tomaszewski M, Kumari M, et al. Blood pressure loci identified with a gene-centric array. *Am J Hum Genet.* 2011;89(6):688-700.
19. Saleem M, Hodgkinson CP, Xiao L, Gimenez-Bastida JA, Rasmussen ML, Foss J, et al. Sox6 as a new modulator of renin expression in the kidney. *Am J Physiol Renal Physiol.* 2020;318(2):F285-F97.
20. Uebbing S, Gockley J, Reilly SK, Kocher AA, Geller E, Gandotra N, et al. Massively parallel discovery of human-specific substitutions that alter enhancer activity. *Proc Natl Acad Sci U S A.* 2021;118(2).
21. Roadmap Epigenomics C, Kundaje A, Meuleman W, Ernst J, Bilenky M, Yen A, et al. Integrative analysis of 111 reference human epigenomes. *Nature.* 2015;518(7539):317-30.
22. Wang F, Zhang L, Zhang GL, Wang ZB, Cui XS, Kim NH, et al. WASH complex regulates Arp2/3 complex for actin-based polar body extrusion in mouse oocytes. *Scientific reports.* 2014;4:5596.
23. Rana A, Jain S, Puri N, Kaw M, Sirianni N, Eren D, et al. The transcriptional regulation of the human angiotensinogen gene after high-fat diet is haplotype-dependent: Novel insights into the gene-regulatory networks and implications for human hypertension. *PLoS One.* 2017;12(5):e0176373.
24. Kovarik P, Stoiber D, Novy M, and Decker T. Stat1 combines signals derived from IFN-gamma and LPS receptors during macrophage activation. *EMBO J.* 1998;17(13):3660-8.
25. Gomez RA, and Lopez ML. Plasticity of Renin Cells in the Kidney Vasculature. *Curr Hypertens Rep.* 2017;19(2):14.
26. Sauter A, Machura K, Neubauer B, Kurtz A, and Wagner C. Development of renin expression in the mouse kidney. *Kidney Int.* 2008;73(1):43-51.
27. Ganesh SK, Tragante V, Guo W, Guo Y, Lanktree MB, Smith EN, et al. Loci influencing blood pressure identified using a cardiovascular gene-centric array. *Hum Mol Genet.* 2013;22(8):1663-78.
28. Perez-Alcala S, Nieto MA, and Barbas JA. LSox5 regulates RhoB expression in the neural tube and promotes generation of the neural crest. *Development.* 2004;131(18):4455-65.
29. Park JA, and Kim KC. Expression patterns of PRDM10 during mouse embryonic development. *BMB Rep.* 2010;43(1):29-33.
30. Shull LC, Sen R, Menzel J, Goyama S, Kurokawa M, and Artinger KB. The conserved and divergent roles of Prdm3 and Prdm16 in zebrafish and mouse craniofacial development. *Dev Biol.* 2020;461(2):132-44.
31. Ding HL, Clouthier DE, and Artinger KB. Redundant roles of PRDM family members in zebrafish craniofacial development. *Developmental dynamics : an official publication of the American Association of Anatomists.* 2013;242(1):67-79.
32. Rahman MM, Kim IS, Ahn D, Tae HJ, and Park BY. PR domaincontaining protein 12 (prdm12) is a downstream target of the transcription factor zic1 during cellular

differentiation in the central nervous system: PR domain containing protein is the right form. *Int J Dev Neurosci.* 2020;80(6):528-37.
33. Asada N, Takase M, Nakamura J, Oguchi A, Asada M, Suzuki N, et al. Dysfunction of fibroblasts of extrarenal origin underlies renal fibrosis and renal anemia in mice. *J Clin Invest.* 2011;121(10):3981-90.
34. Kemmner S, Bachmann Q, Steiger S, Lorenz G, Honarpisheh M, Foresto-Neto O, et al. STAT1 regulates macrophage number and phenotype and prevents renal fibrosis after ischemia-reperfusion injury. *Am J Physiol Renal Physiol.* 2019;316(2):F277-F91.
35. Pattanaik D, Brown M, Postlethwaite BC, and Postlethwaite AE. Pathogenesis of Systemic Sclerosis. *Front Immunol.* 2015;6:272.
36. Flister MJ, Tsaih SW, O'Meara CC, Endres B, Hoffman MJ, Geurts AM, et al. Identifying multiple causative genes at a single GWAS locus. *Genome Res.* 2013;23(12):1996-2002.
37. Sparks MA, Crowley SD, Gurley SB, Mirotsou M, and Coffman TM. Classical Renin-Angiotensin system in kidney physiology. *Compr Physiol.* 2014;4(3):1201-28.
38. Jones CA, Sigmund CD, McGowan RA, Kane-Haas CM, and Gross KW. Expression of murine renin genes during fetal development. *Mol Endocrinol.* 1990;4(3):375-83.
39. Sequeira Lopez ML, Pentz ES, Robert B, Abrahamson DR, and Gomez RA. Embryonic origin and lineage of juxtaglomerular cells. *Am J Physiol Renal Physiol.* 2001;281(2):F345-56.
40. Humphreys BD, Lin SL, Kobayashi A, Hudson TE, Nowlin BT, Bonventre JV, et al. Fate tracing reveals the pericyte and not epithelial origin of myofibroblasts in kidney fibrosis. *Am J Pathol.* 2010;176(1):85-97.
41. Kuppe C, Ibrahim MM, Kranz J, Zhang X, Ziegler S, Perales-Paton J, et al. Decoding myofibroblast origins in human kidney fibrosis. *Nature.* 2021;589(7841):281-6.
42. Kent WJ, Sugnet CW, Furey TS, Roskin KM, Pringle TH, Zahler AM, et al. The human genome browser at UCSC. *Genome Res.* 2002;12(6):996-1006.
43. Frankish A, Diekhans M, Ferreira AM, Johnson R, Jungreis I, Loveland J, et al. GENCODE reference annotation for the human and mouse genomes. *Nucleic Acids Res.* 2019;47(D1):D766-D73.
44. Kim D, Pertea G, Trapnell C, Pimentel H, Kelley R, and Salzberg SL. TopHat2: accurate alignment of transcriptomes in the presence of insertions, deletions and gene fusions. *Genome Biol.* 2013;14(4):R36.
45. Trapnell C, Roberts A, Goff L, Pertea G, Kim D, Kelley DR, et al. Differential gene and transcript expression analysis of RNA-seq experiments with TopHat and Cufflinks. *Nat Protoc.* 2012;7(3):562-78.
46. Ran FA, Hsu PD, Wright J, Agarwala V, Scott DA, and Zhang F. Genome engineering using the CRISPR-Cas9 system. *Nat Protoc.* 2013;8(11):2281-308.
47. Gunawardhana KL, and Hardin PE. VRILLE Controls PDF Neuropeptide Accumulation and Arborization Rhythms in Small Ventrolateral Neurons to Drive Rhythmic Behavior in Drosophila. *Curr Biol.* 2017;27(22):3442-53 e4.
48. Gunawardhana KL, Rivas GBS, Caster C, and Hardin PE. Crosstalk between vrille transcripts, proteins, and regulatory elements controlling circadian rhythms and development in Drosophila. *iScience.* 2021;24(1):101893.

49. Tso CF, Simon T, Greenlaw AC, Puri T, Mieda M, and Herzog ED. Astrocytes Regulate Daily Rhythms in the Suprachiasmatic Nucleus and Behavior. *Curr Biol.* 2017;27(7):1055-61.

Figure and Tables

SNP ID	**Aorta**		**Tibial Artery.**	
	NES	p-value	NES	P-value
rs555626	-0.124	3.4e-3	-	-
rs2287696	-0.124	4.1e-4	-0.164	2.7e-7
rs1422279	-0.086	3.4e-4	-0.0948	1.6e-5
Rs13359291	-0.115	5.7e-4	-0.161	1.2e-7

Table 1. GWAS variants for hypertension that are eQTL for *PRDM6* in the tibial artery and aorta

SNP ID	Position	Tested bp change	Abs. Differential Activation	P-values
rs458158;rs335170	123146486;123146548	C:A;A:C	0.871983	0.002134
rs458158	123146486	C:A	0.952735	0.002903
rs374621;rs480764;rs589928	123144566;123144580;123144622	G:A;C:T;C:G	0.199138	0.005308
rs888858;rs5871031	123151695;123151726	T:C	0.12941	0.005791
rs6862547	123112617	A:G	0.139749	0.008976
rs602648;rs412232;rs61698607	123137494;123137503;123137558	A:T;A:G;T:C	0.28111	0.009307
rs374621;rs589928	123144566;123144622	G:A;C:G	0.09582	0.010143
rs394782;rs5871031	123151709;123151726	T:C	0.210647	0.010327
rs10077410	123115075	G:A	0.297527	0.01163
rs394782	123151709	T:C	0.05531	0.014083
rs10044090;rs335158	123140031;123140083	T:C;G:A	2.288728	0.015108
rs457807	123117723	G:C	0.12497	0.020125
rs602648;rs61698607	123137494;123137558	A:T;T:C	0.32886	0.022348
rs335147	123109141	T:C	0.14705	0.022617
rs457807;rs34901094	123117723;123117778	G:C;T:-	0.008536	0.023068
rs374621;rs589928	123144566;123144622	G:A;C:G	0.213332	0.024018
rs464106	123109600	A:G	0.013774	0.024499
rs182432601;rs459678;rs459638	123122145;123122161;123122212	G:A;G:A;G:A	0.311318	0.025439
rs335184;rs73294789	123113120;123113145	A:G;A:G	0.231136	0.025464
rs335147;rs200104783	123109141;123109206	T:C;C:A	0.15042	0.027427
rs335170	123146548	A:C	0.568737	0.028633
rs151031477;rs112009226	123111712;123111715	A:C	0.06454	0.029108
rs651304;rs112009226;rs73294785	123111691;123111715;123111779	C:G;A:C;C:G	0.05617	0.031092
rs13359291	123140762	G:A	0.302568	0.032351
rs374621	123144566	G:A	0.16263	0.035954
rs602648;rs412232	123137494;123137503	A:T;A:G	0.33791	0.038018
rs145044129	123119173	AAAC:-	0.58506	0.041316
rs459638	123122212	G:A	0.153895	0.04337
rs337127	123105337	C:G	0.188342	0.044274
rs651304;rs112009226	123111691;123111715	C:G;A:C	0.005381	0.046619
rs337136;rs35911138	123111437;123111505	T:C;A:G	0.09313	0.047195
rs457807;rs189191;rs34901094	123117723;123117724;123117778	G:C;C:G;T:-	0.14367	0.04801
rs368699046	123125061		0.10734	0.048077
rs335186;rs181518726;rs113757571	123111589;123111591;123111643	C:G;G:A;T:G	0.333126	0.04814
rs189191;rs34901094	123117724;123117778	C:G;T:-	0.20243	0.048168
rs10519718	123117863	A:T	0.23486	0.049225
rs233174	123147447	G:A	0.1404	0.04971

Table 2. MPRA results summarizing the allele-specific activity of CREs which showed significant allele-specific activity are presented (p-value < 0.05). For each CRE, associated SNP IDs, genomic position, tested alleles, differential activation potential, and the p-value is indicated.

SNP	rs457807	rs459638	rs10044090	rs459678	rs335158	rs368699046
rs13359291			0.9971		1.0000	1.0000
rs555625	0.9740	0.9913		0.9913		
rs2287696						1.0000

Table 3. Linkage disequilibrium between GWAS leads SNPs and SNPs with differential expression in MPRA. The pairwise LD values for each SNP combination with R^2>0.9 are represented.

SNP Names	Position	BP	p	LD	dAct	Putative TF
rs13359291	123140763	G:A	0.03	Lead SNP	0.3	CEBP beta and alpha
rs10044090	123140032	T:C	0.015	rs13359291	2.28	c-Myb
rs335158	123140084	G:A				
rs457807	123117724	G:C	0.02	rs555625	-0.12	ENKTF-1/ FOXP3(binds the alt. allele)
rs459638	123122213	G:A	0.04	rs555625	0.15	ZNF366
rs459638	123122213	G:A	0.02	rs555625	0.31	ZNF366
rs459678	123122162	G:A		rs555625		c-Jun/ATF3
rs182432601	123122146	G:A		----------		

Table 4 Putative transcription factors at specific SNP loci

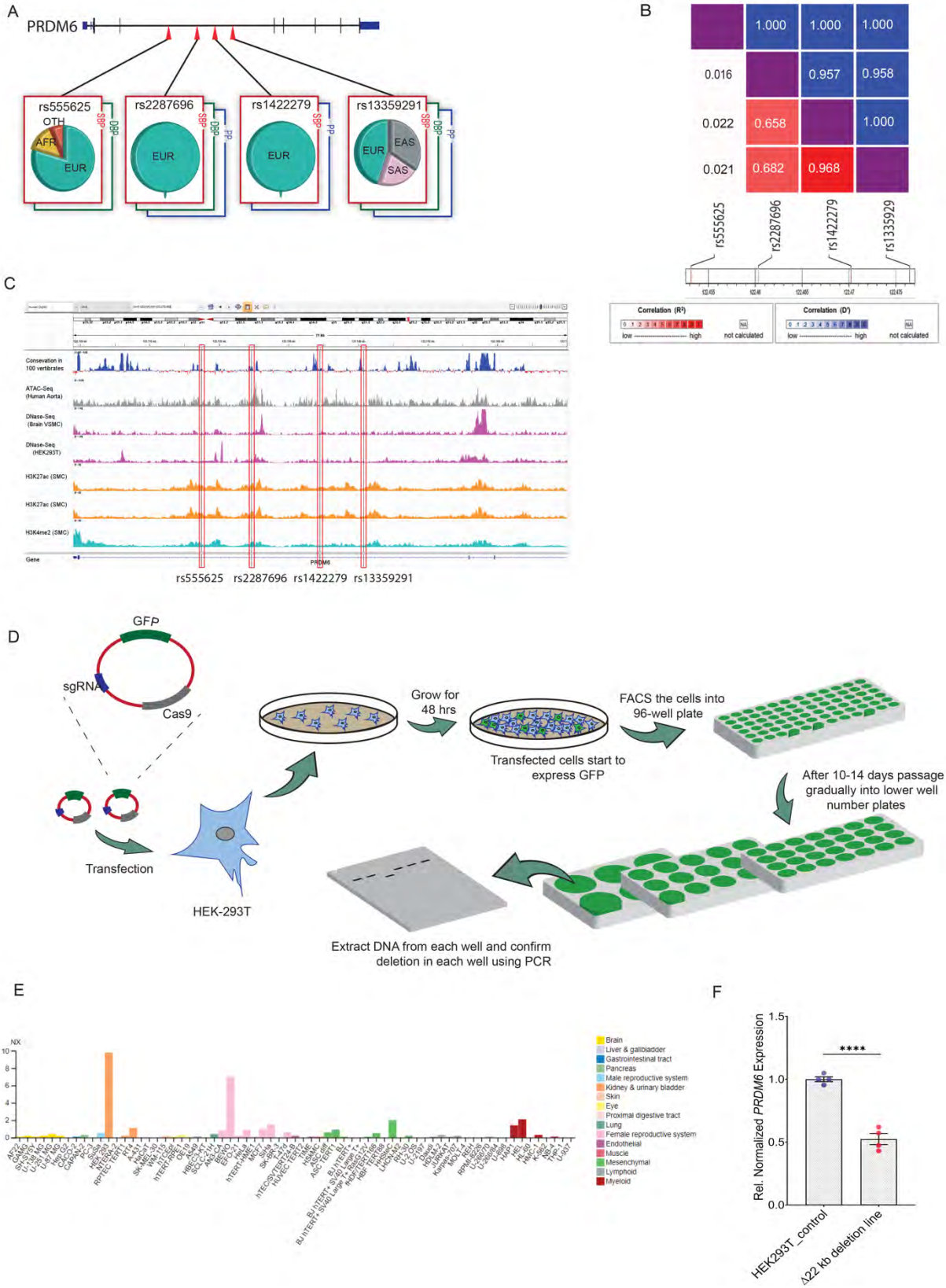
A
PRDM6
rs555625
OTH
AFR
EUR
SBP
DBP
rs2287696
EUR
PP
rs1422279
EUR
rs13359291
EUR
EAS
SAS
B
1.000
1.000
1.000
0.016
0.957
0.958
0.022
0.658
1.000
0.021
0.682
0.968
rs555625
rs2287696
rs1422279
rs1335929
Correlation (R²)
low
high
not calculated
Correlation (D')
C
Conservation in 100 vertebrates
ATAC-Seq (Human Aorta)
DNase-Seq (Brain VSMC)
DNase-Seq (HEK293T)
H3K27ac (SMC)
H3K27ac (SMC)
H3K4me2 (SMC)
Gene
PRDM6
rs555625 rs2287696 rs1422279 rs13359291
D
GFP
sgRNA
Cas9
Transfection
HEK-293T
Grow for 48 hrs
Transfected cells start to express GFP
FACS the cells into 96-well plate
After 10-14 days passage gradually into lower well number plates
Extract DNA from each well and confirm deletion in each well using PCR
E
NX
Brain
Liver & gallbladder
Gastrointestinal tract
Pancreas
Male reproductive system
Kidney & urinary bladder
Skin
Eye
Proximal digestive tract
Lung
Female reproductive system
Endothelial
Muscle
Mesenchymal
Lymphoid
Myeloid
F
Rel. Normalized PRDM6 Expression
1.5
1.0
0.5
0.0
****
HEK293T_control
Δ22 kb deletion line

Figure 1. GWAS lead SNPs in PRDM6 intron 3 and their CRISPR deletion A) Genetic variants in PRDM6 gene discovered by GWAS of blood pressure B) LD structure of rs13359291, rs2287696, rs1422279 and rs555625 in the East Asian population. R^2 and D' for each SNP pair is represented inside corresponding boxes C) Relationship between lead SNPs and open chromatin regions and histone marks. (sources: ATAC-Seq – doi:10.17989/ENCSR344ZTM, DNase-Seq (brain VSMC) – doi:10.17989/ENCSR000ENG, DNase-Seq (HEK293T) – doi:10.17989/ENCSR000EJR, H3K27ac – doi:10.17989/ENCSR210ZPC, H3K4me2– doi:10.17989/ENCSR783AXV) D) schematic of CRISPR-Cas9-mediated deletion of the ~22 kb LD region in intron 3, encompassing all lead SNPs, HEK293T, n=4 technical replicates E) Expression of PRDM6 in different human cell lines (source: www.proteinatlas.org/). F) Significant reduction of *PRDM6* mRNA expression upon deletion of the LD region compared to the wild-type sequence assayed by RT-qPCR, identifying the intronic region as an enhancer locus for PRDM6. n=4. Unpaired t-test, 2-sided, n=4 technical replicates. **** specifies $p<0.0001$. SBP – systolic blood pressure, DBP – diastolic blood pressure, PP – pulse pressure, NES – normalized effect size

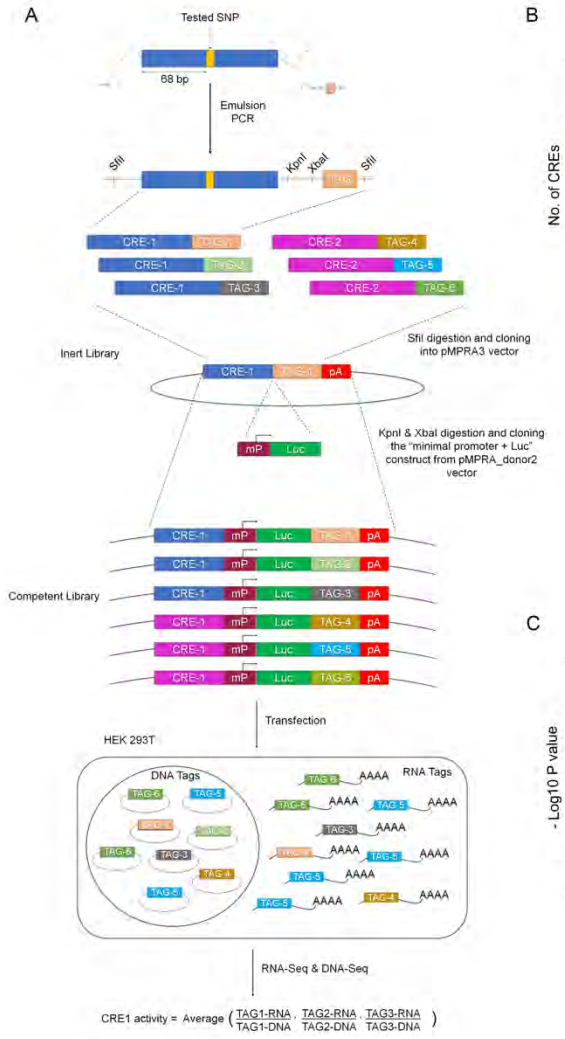
A
Tested SNP
68 bp
Emulsion PCR
SfiI
KpnI
XbaI
SfiI
CRE-1
TAG-1
CRE-2
TAG-4
CRE-1
TAG-2
CRE-2
TAG-5
CRE-1
TAG-3
CRE-2
TAG-6
Inert Library
SfiI digestion and cloning into pMPRA3 vector
CRE-1
TAG-1
pA
mP
Luc
KpnI & XbaI digestion and cloning the "minimal promoter + Luc" construct from pMPRA_donor2 vector
Competent Library
CRE-1
mP
Luc
TAG-1
pA
CRE-1
mP
Luc
TAG-2
pA
CRE-1
mP
Luc
TAG-3
pA
CRE-1
mP
Luc
TAG-4
pA
CRE-1
mP
Luc
TAG-5
pA
CRE-1
mP
Luc
TAG-6
pA
Transfection
HEK 293T
DNA Tags
RNA Tags
RNA-Seq & DNA-Seq
CRE1 activity = Average (TAG1-RNA / TAG1-DNA , TAG2-RNA / TAG2-DNA , TAG3-RNA / TAG3-DNA)

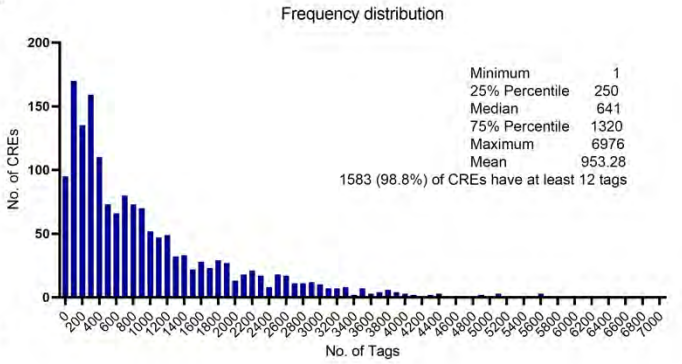
B
Frequency distribution
Minimum 1
25% Percentile 250
Median 641
75% Percentile 1320
Maximum 6976
Mean 953.28
1583 (98.8%) of CREs have at least 12 tags
No. of CREs
No. of Tags

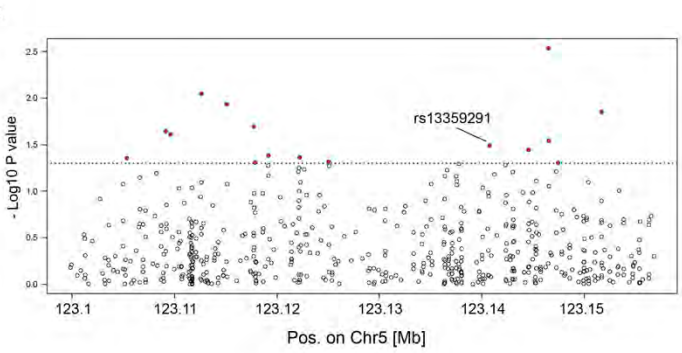
C
rs13359291
- Log10 P value
Pos. on Chr5 [Mb]

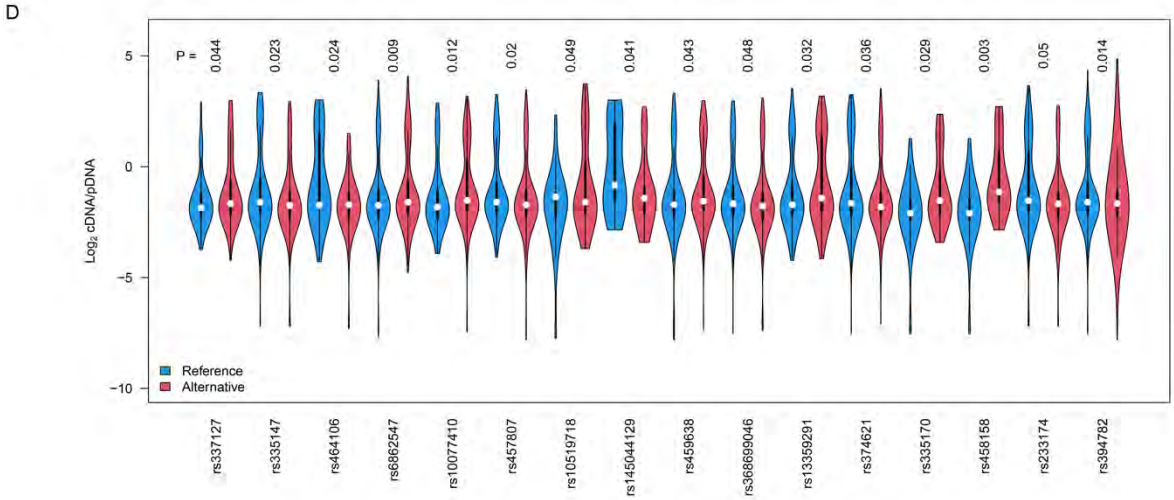
D
P =
0.044
0.023
0.024
0.009
0.012
0.02
0.049
0.041
0.043
0.048
0.032
0.036
0.029
0.003
0.05
0.014
Log2 cDNA/pDNA
Reference
Alternative
rs337127
rs335147
rs464106
rs6862547
rs10077410
rs457807
rs10519718
rs145044129
rs459638
rs368699046
rs13359291
rs374621
rs335170
rs458158
rs233174
rs394782

Figure 2. Massively Parallel Reporter Assay (MPRA) of PRDM6 intron 3 variants A) The schematic of MPRA of 336 common variants in the 3rd intron of PRDM6 from generation of inert and competent libraries, cloning into MPRA vectors, transfection into HEK293T cells and RNA & DNA sequencing and analysis B) Frequency distribution of bar graphs showing the number of tags associated with each MPRA fragment. Distribution statistics are represented. C) Manhattan plot showing sixteen single SNPs which significantly altered the gene expression due to a single base pair change with MPRA. D) violin plots of the sixteen single SNPs showing allele-specific expression of the reporter gene. Statistics were carried out using One-Way Anova. $p<0.05$ was considered significant.

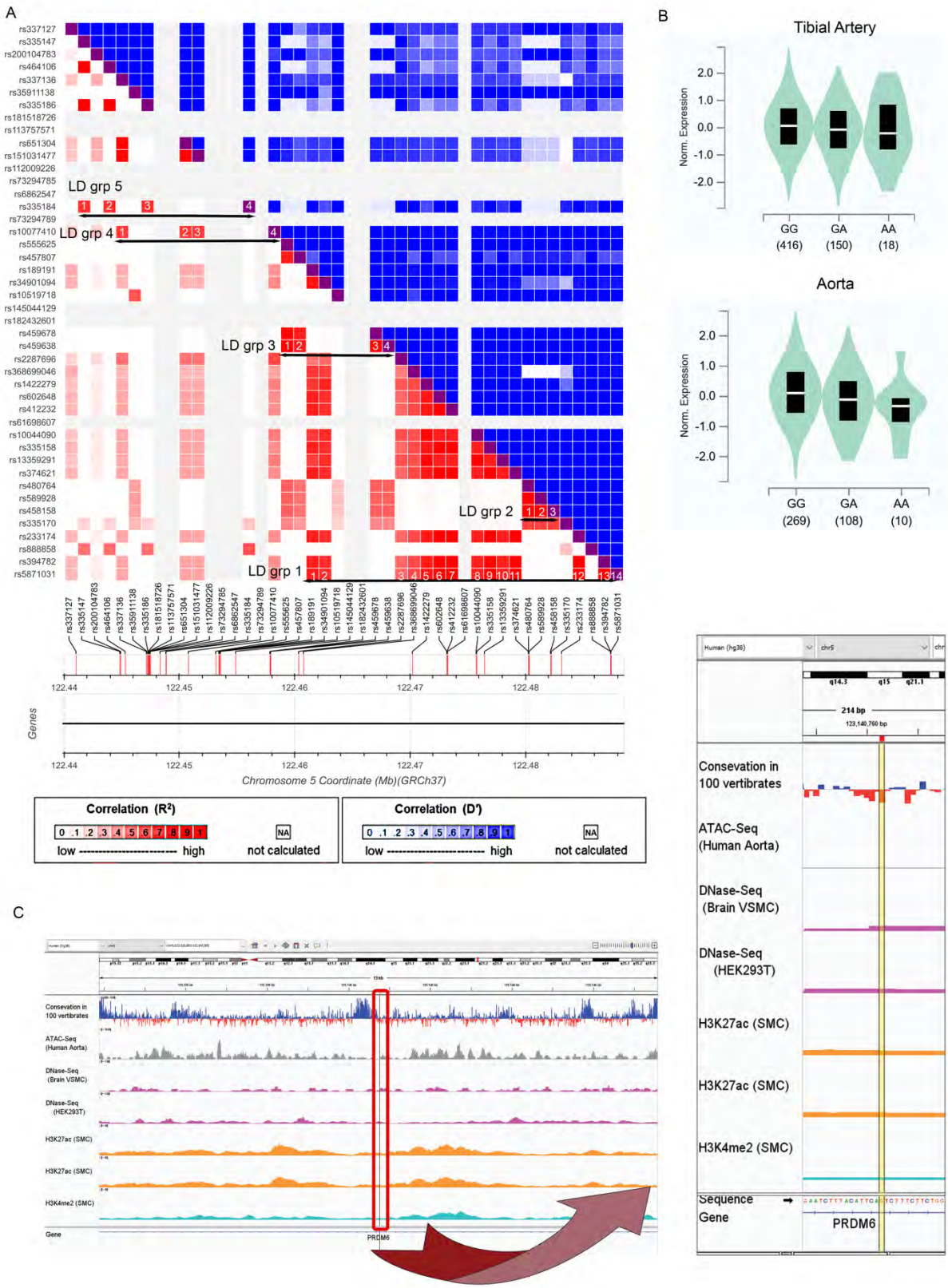
A
LD grp 5
LD grp 4
LD grp 3
LD grp 2
LD grp 1
Genes
Chromosome 5 Coordinate (Mb)(GRCh37)
Correlation (R²)
low ---------- high
not calculated
Correlation (D')
low ---------- high
not calculated
B
Tibial Artery
Norm. Expression
GG (416)
GA (150)
AA (18)
Aorta
GG (269)
GA (108)
AA (10)
C
Consevation in 100 vertibrates
ATAC-Seq (Human Aorta)
DNase-Seq (Brain VSMC)
DNase-Seq (HEK293T)
H3K27ac (SMC)
H3K27ac (SMC)
H3K4me2 (SMC)
Gene
PRDM6
Sequence
Gene

Figure 3. CRISPR deletion of SNPs with altered allele-specific expression and their location in different haplotypes A) Five different LD groups (R^2>0.70) in the East Asian population based on the haplotypes generated from lead GWAS SNPs and SNPs discovered by the MPRA B) violin plots showing *PRDM6* expression in the tibial artery and aorta with different allelic combinations pertinent to rs13359291 (source: GTEx database) C) location of the rs13359291 in relationship to open chromatin region of the aorta and histone markers and the sequence conservation in 100 vertebrates. The SNP region is zoomed in for clarity

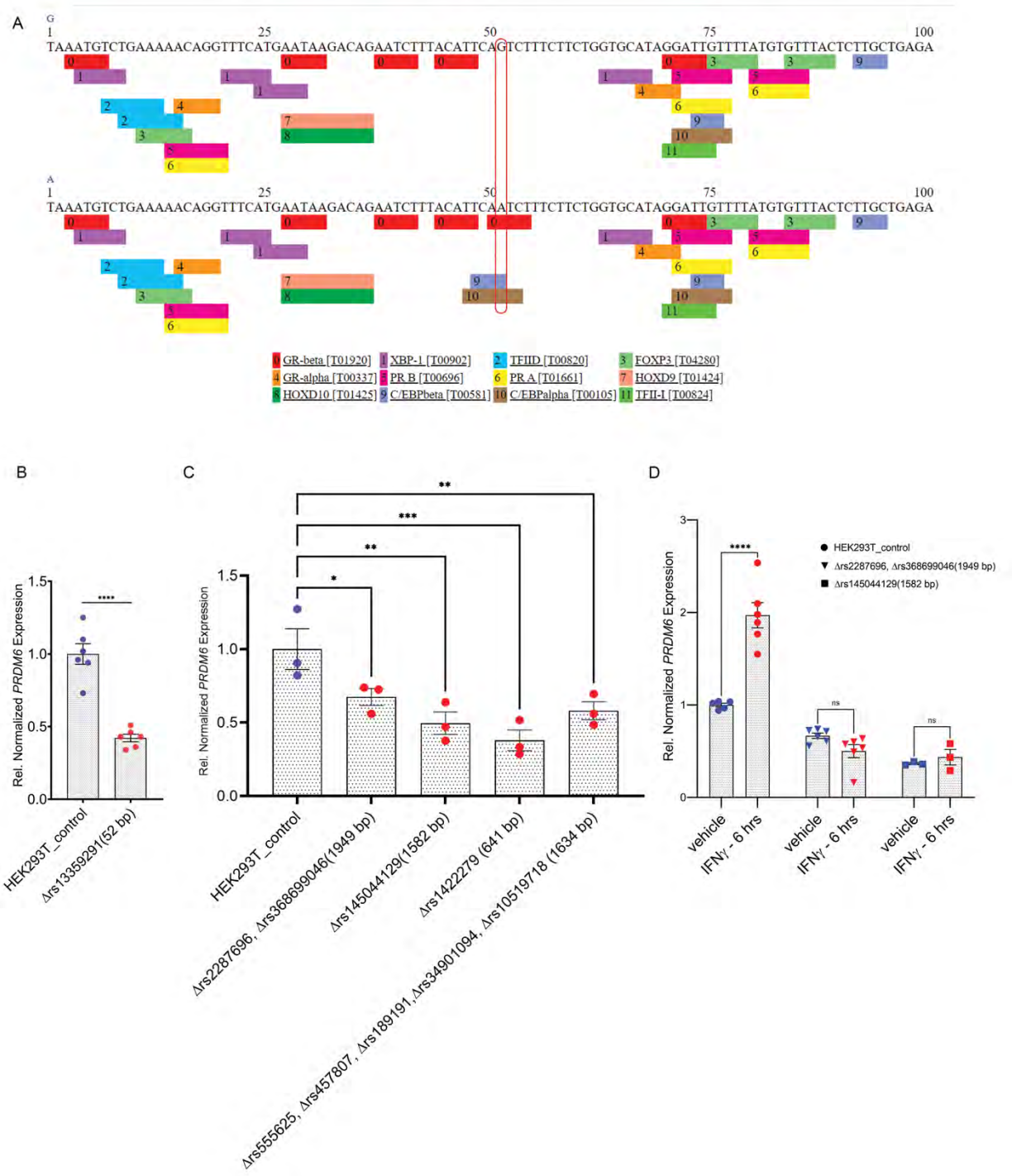

Figure 4. A) Putative binding site for CEBP beta and alpha based on PROMO silico motif finder, B) Downregulation in *PRDM6* mRNA expression in the 52 bp CRISPR-Cas9-deletion encompassing rs13359291 compared to wild-type cells by RT-qPCR. C) Downregulation in *PRDM6* mRNA expression in the depicted sized CRISPR-Cas9-deletions encompassing the mentioned SNPs, compared to wild-type cells by RT-qPCR. n>3 independent replicates. ***p<0.001, **p<0.01, *p<0.05. D) IFNγ stimulation of HEK293T cells with and without

CRISPR deletions encompassing STAT1 binding regions. Unpaired t-test or One-Way Anova. **** specifies $p<0.0001$, ***$p<0.001$. $n>3$ independent replicates.

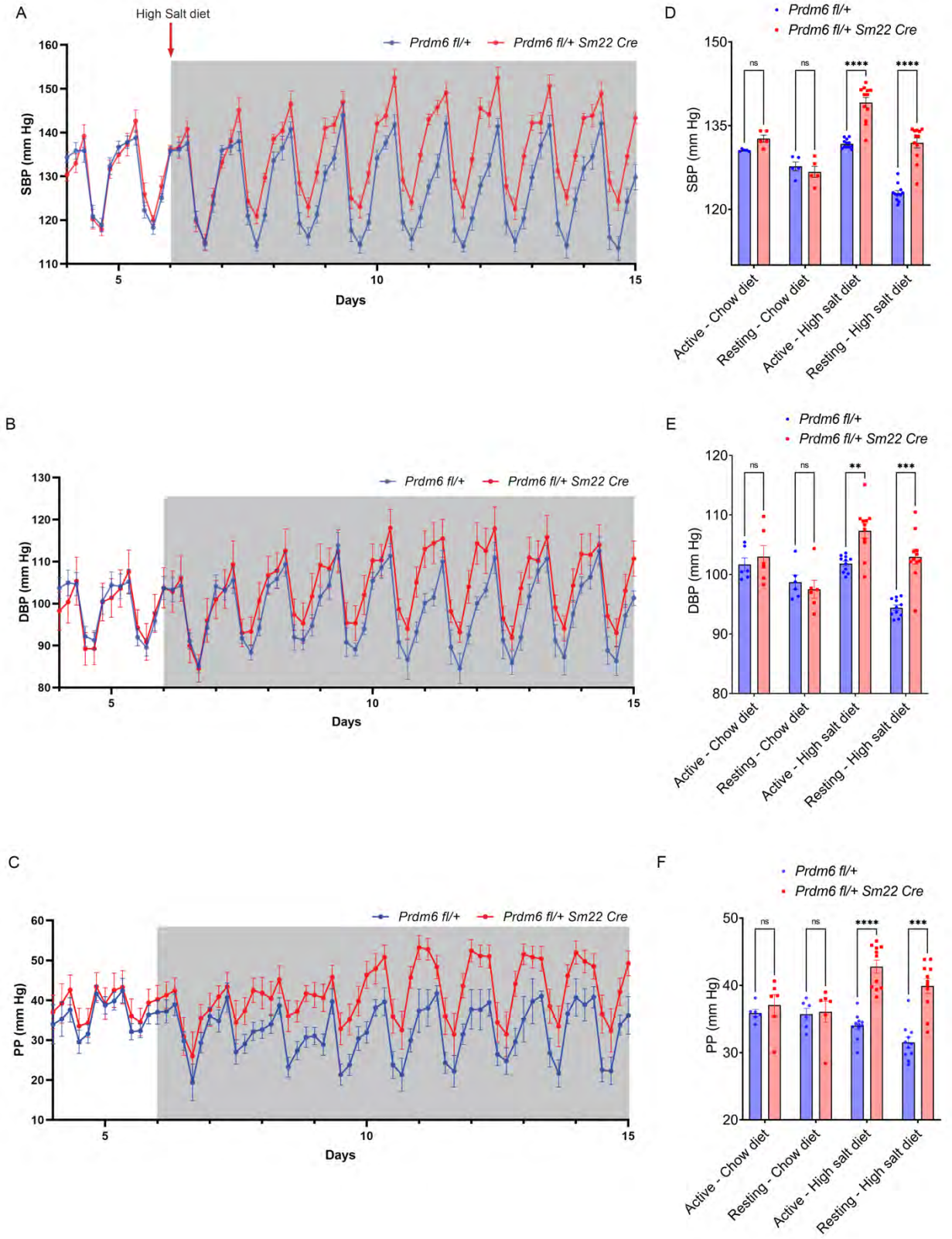

Figure 5. Invasive measurement of blood pressure indices in *Prdm6fl+ Sm22Cre* and wild-type mice A -C) systolic BP (SBP), diastolic BP (DBP), and pulse pressure (PP) of *Prdm6fl+*

Sm22Cre and *Prdm6fl+* mice. Mice were on a chow diet (day 4-5) and a high salt diet (day 6-14). D-F) Changes of all three traits during the resting (daytime) and active (nighttime) phases under different dietary conditions. Multiple paired t-test, 2-sided. **** specifies adjusted $p<0.0001$, *** is adjusted $p<0.001$. $n>5$-11 mice per group

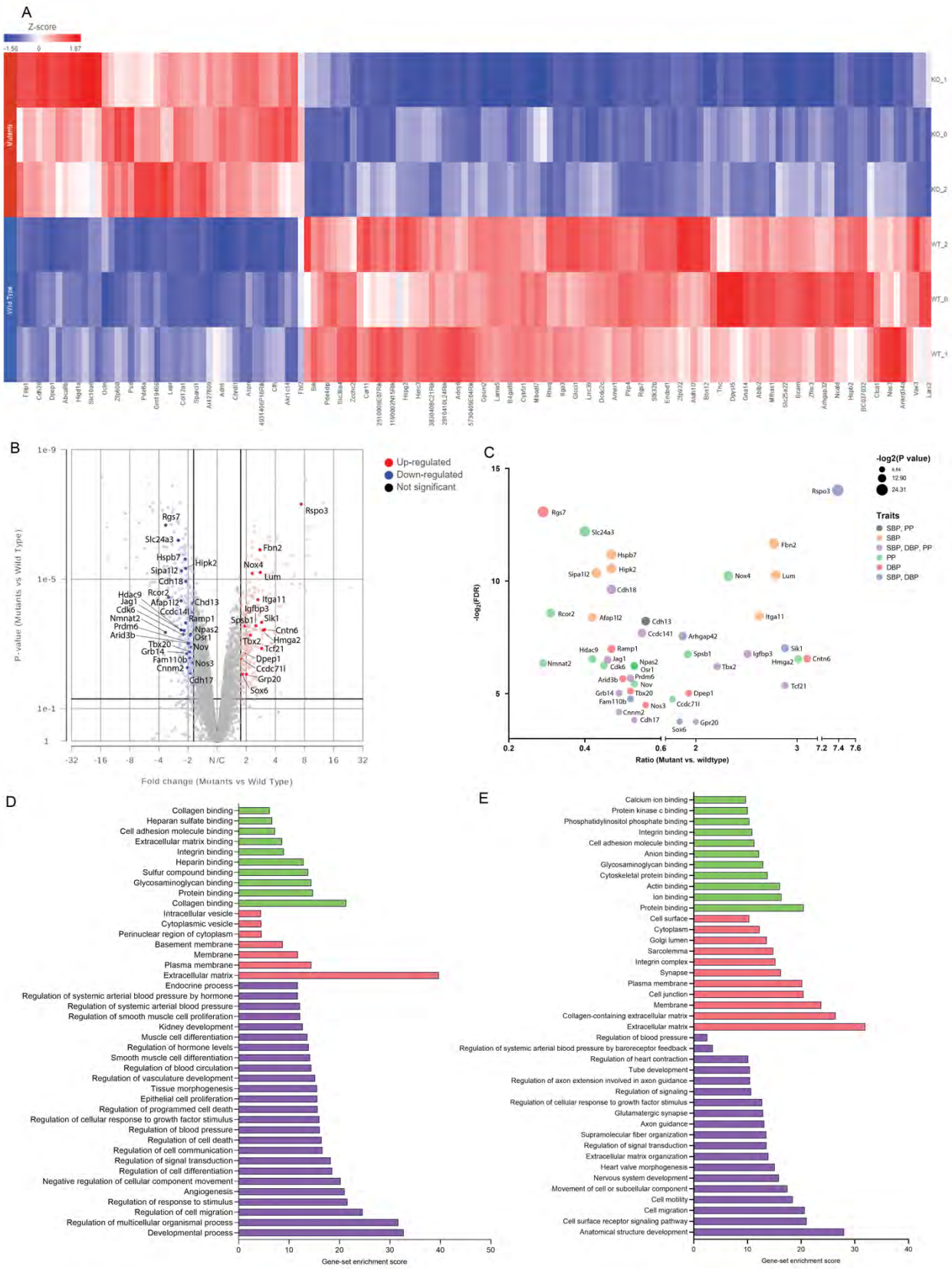
A
Z-score
-1.56
0
1.87
Mutants
Wild Type
KO_1
KO_0
KO_2
WT_2
WT_0
WT_1
B
Up-regulated
Down-regulated
Not significant
P-value (Mutants vs Wild Type)
Fold change (Mutants vs Wild Type)
Rspo3
Rgs7
Slc24a3
Fbn2
Hspb7
Hipk2
Nox4
Sipa1l2
Lum
Cdh18
Itga11
Igfbp3
Slk1
Cntn6
Hmga2
Tcf21
Dpep1
Ccdc71l
Grp20
Sox6
Cdh17
Nos3
Nov
Osr1
Npas2
Ramp1
Spsb1
Tbx2
Tbx20
Grb14
Fam110b
Cnnm2
Chd13
Afap1l2
Ccdc141
Jag1
Cdk6
Nmnat2
Prdm6
Arid3b
Hdac9
Rcor2
C
-log2(P value)
Traits
SBP, PP
SBP
SBP, DBP, PP
PP
DBP
SBP, DBP
-log2(FDR)
Ratio (Mutant vs. wildtype)
Arhgap42
D
Collagen binding
Heparan sulfate binding
Cell adhesion molecule binding
Extracellular matrix binding
Integrin binding
Heparin binding
Sulfur compound binding
Glycosaminoglycan binding
Protein binding
Intracellular vesicle
Cytoplasmic vesicle
Perinuclear region of cytoplasm
Basement membrane
Membrane
Plasma membrane
Extracellular matrix
Endocrine process
Regulation of systemic arterial blood pressure by hormone
Regulation of systemic arterial blood pressure
Regulation of smooth muscle cell proliferation
Kidney development
Muscle cell differentiation
Regulation of hormone levels
Smooth muscle cell differentiation
Regulation of blood circulation
Regulation of vasculature development
Tissue morphogenesis
Epithelial cell proliferation
Regulation of programmed cell death
Regulation of cellular response to growth factor stimulus
Regulation of blood pressure
Regulation of cell death
Regulation of cell communication
Regulation of signal transduction
Regulation of cell differentiation
Negative regulation of cellular component movement
Angiogenesis
Regulation of response to stimulus
Regulation of cell migration
Regulation of multicellular organismal process
Developmental process
Gene-set enrichment score
E
Calcium ion binding
Protein kinase c binding
Phosphatidylinositol phosphate binding
Integrin binding
Cell adhesion molecule binding
Anion binding
Glycosaminoglycan binding
Cytoskeletal protein binding
Actin binding
Ion binding
Protein binding
Cell surface
Cytoplasm
Golgi lumen
Sarcolemma
Integrin complex
Synapse
Plasma membrane
Cell junction
Membrane
Collagen-containing extracellular matrix
Extracellular matrix
Regulation of blood pressure
Regulation of systemic arterial blood pressure by baroreceptor feedback
Regulation of heart contraction
Tube development
Regulation of axon extension involved in axon guidance
Regulation of signaling
Regulation of cellular response to growth factor stimulus
Glutamatergic synapse
Axon guidance
Supramolecular fiber organization
Regulation of signal transduction
Extracellular matrix organization
Heart valve morphogenesis
Nervous system development
Movement of cell or subcellular component
Cell motility
Cell migration
Cell surface receptor signaling pathway
Anatomical structure development
Gene-set enrichment score

Figure 6. RNA-Seq analysis of *Prdm6fl/fl Sm22Cre* mice aortic tissue A) RNA-Seq hit map of homozygous SMC-specific knockout (*Prdm6fl/fl Sm22Cre*) mice aortic tissue and their littermate controls at P0.5. 349 of the genes were upregulated while 769 genes were downregulated in *Prdm6fl/fl Sm22Cre* vs. wild-type mice aortas. B) Volcano plot demonstrating genes with significantly altered expression in *Prdm6fl/fl Sm22Cre* mice aorta vs. wild-type mice aorta; the plot shows fold change vs. p-value; a selected number of genes associated with hypertension are annotated C) A bubble plot representing aforementioned genes associated with different BP traits (SBP: Systolic BP, DBP: Diastolic BP and PP: Pulse pressure). D-E). Gene-set enrichment analyses show many blood pressure-related processes to be significantly enriched in both up D) and down-regulated E) genes.

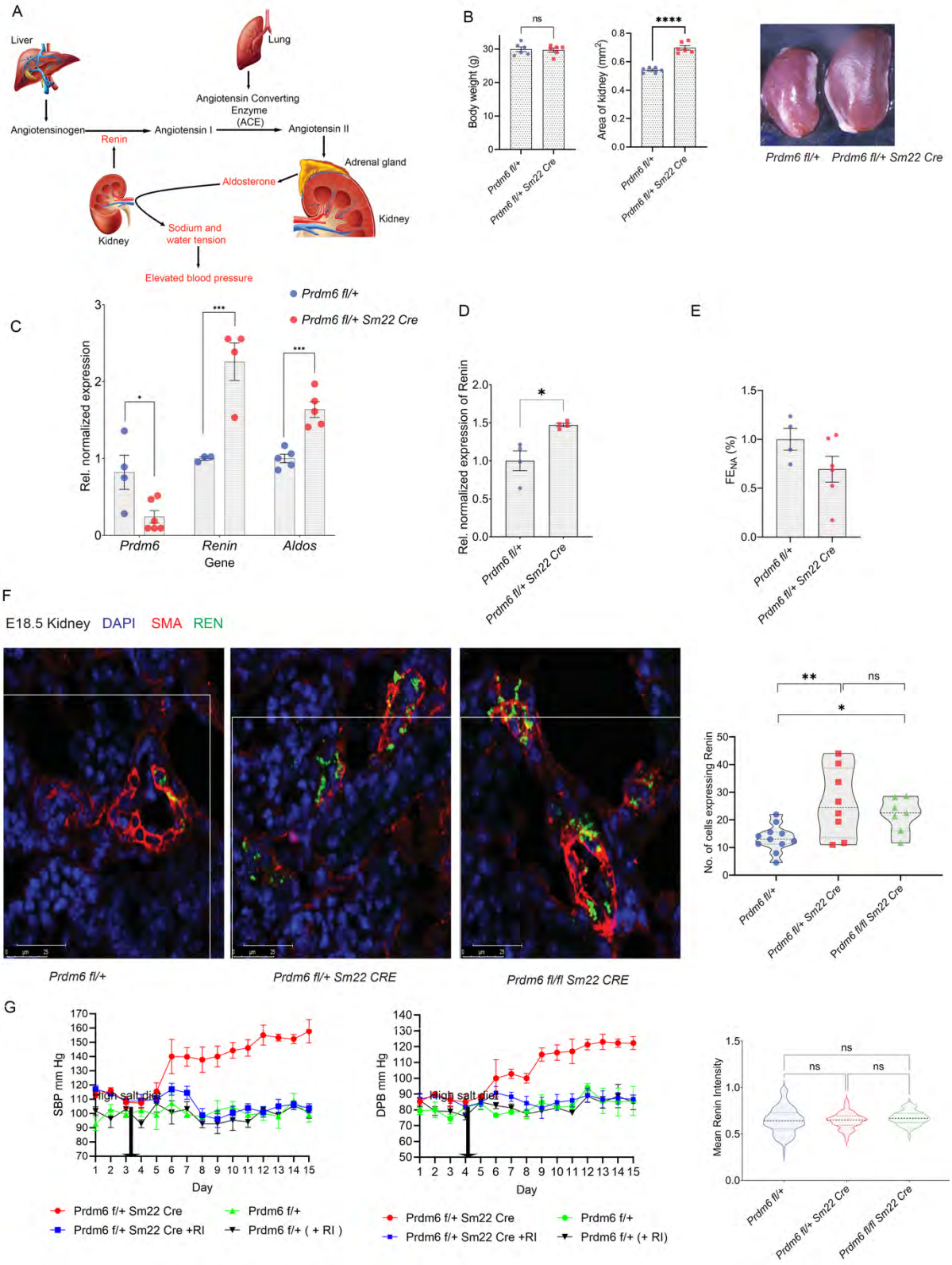
A
Liver
Lung
Angiotensin Converting Enzyme (ACE)
Angiotensinogen
Renin
Angiotensin I
Angiotensin II
Adrenal gland
Aldosterone
Kidney
Kidney
Sodium and water tension
Elevated blood pressure
B
ns
****
Body weight (g)
Area of kidney (mm2)
Prdm6 fl/+
Prdm6 fl/+ Sm22 Cre
Prdm6 fl/+ Prdm6 fl/+ Sm22 Cre
C
Prdm6 fl/+
Prdm6 fl/+ Sm22 Cre
Rel. normalized expression
Prdm6
Renin
Aldos
Gene
D
Rel. normalized expression of Renin
E
FENA (%)
F
E18.5 Kidney DAPI SMA REN
Prdm6 fl/+
Prdm6 fl/+ Sm22 CRE
Prdm6 fl/fl Sm22 CRE
No. of cells expressing Renin
Prdm6 fl/fl Sm22 Cre
G
SBP mm Hg
DPB mm Hg
High salt diet
Day
Prdm6 f/+ Sm22 Cre
Prdm6 f/+ Sm22 Cre +RI
Prdm6 f/+
Prdm6 f/+ (+ RI)
Prdm6 f/+ (+ RI)
Mean Renin Intensity

Figure 7. The increase in renin-producing cells and renin-aldosterone expression in *Prdm6fl/+ Sm22Cre* mice A) Schematic of renin-angiotensin-aldosterone axis regulation. B) Comparison of body weight and area of kidney between *Prdm6fl/+ Sm22Cre* and wild-type mice. n=6 mice per group C-D) Higher renin mRNA and protein levels in the kidneys and aldosterone synthase mRNA levels in the adrenal glands of adult *Prdm6fl/+ Sm22Cre* mice vs. wild-type littermates n=4-6 mice per group. Below the western blot is the quantification of the blot, normalized Renin expression to Gapdh. n=4 mice per group E) The fraction of sodium excretion (FE_{NA}) in *Prdm6fl/+ Sm22Cre* vs. wild-type mice. n=4-5 mice per group F) Renin protein levels in E18.5 kidney of *Prdm6fl/+ Sm22Cre* and *Prdm6fl/fl Sm22Cre* mice and their corresponding wild-type littermates by immunofluorescence staining. G) The number of Renin-expressing cells per fixed area for all three genotypes. n=7 mice per group H) Mean Renin intensity for the mentioned genotypes. I) Systolic and diastolic blood pressure measurements in *Prdm6fl/+ Sm22Cre* and wild-type mice on a high salt diet with and without treatment with aliskiren. n>6 mice per group. Data are shown as mean $\pm$ SEM. Kruskal-Wallis One-way ANOVA **** specifies $p<0.0001$, ***$p<0.001$, **$p<0.01$, *$p<0.05$.

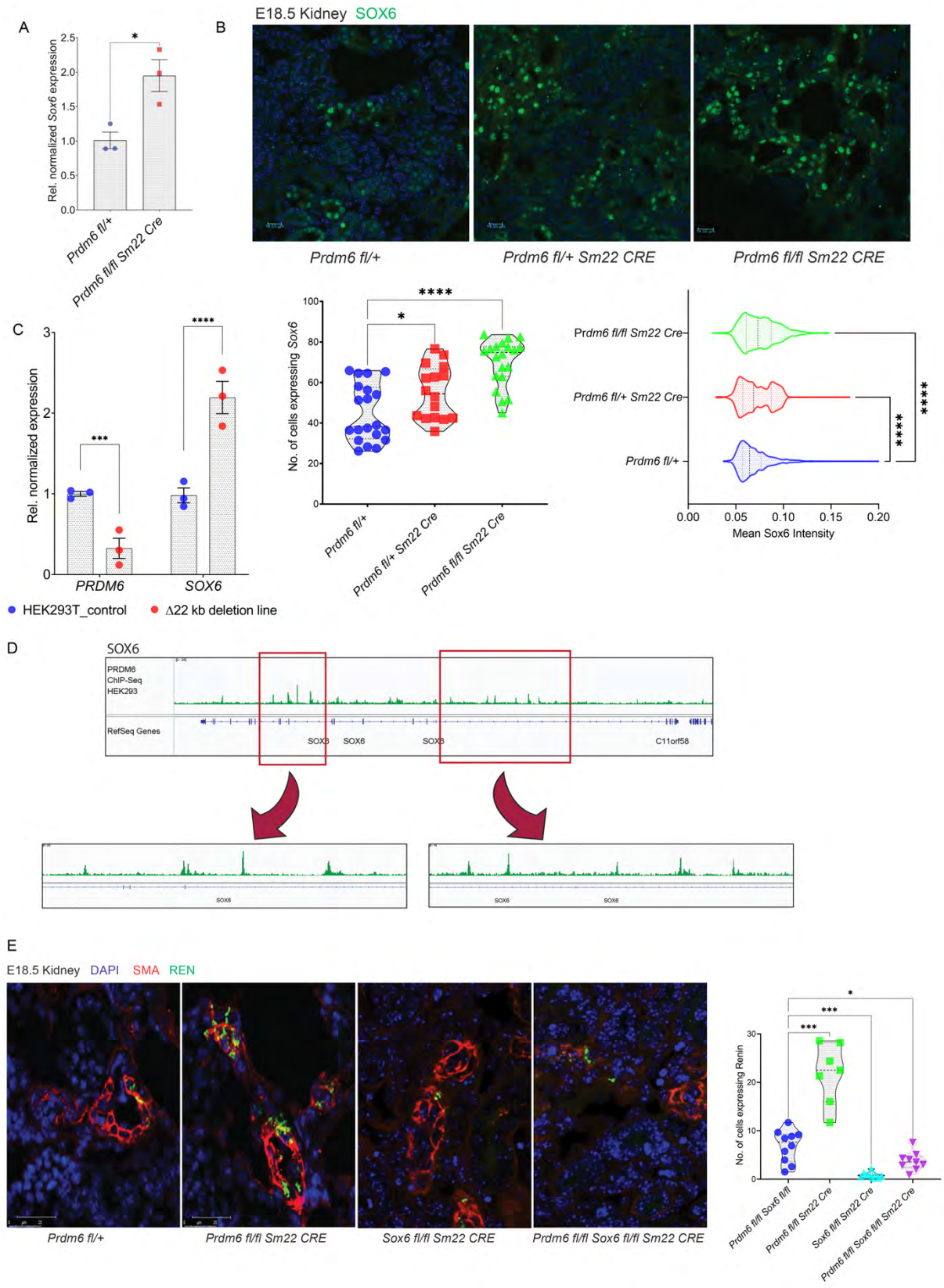
A
Rel. normalized Sox6 expression
Prdm6 fl/+
Prdm6 fl/fl Sm22 Cre
B
E18.5 Kidney SOX6
Prdm6 fl/+
Prdm6 fl/+ Sm22 CRE
Prdm6 fl/fl Sm22 CRE
C
Rel. normalized expression
PRDM6
SOX6
HEK293T_control
Δ22 kb deletion line
No. of cells expressing Sox6
Mean Sox6 Intensity
D
SOX6
PRDM6 ChIP-Seq HEK293
RefSeq Genes
C11orf58
E
E18.5 Kidney DAPI SMA REN
Prdm6 fl/+
Prdm6 fl/fl Sm22 CRE
Sox6 fl/fl Sm22 CRE
Prdm6 fl/fl Sox6 fl/fl Sm22 CRE
No. of cells expressing Renin

Figure 8. *Sox6* is transcriptionally regulated by PRDM6 A) *Sox6* transcript levels in *Prdm6fl/fl Sm22Cre* and wild-type littermate mice aorta (n=3 per group). B) The immunofluorescence staining of Sox6 in heterozygous, homozygous *Prdm6* knockout mice and their wild-type littermates. The number of cells expressing Sox6 (top) and mean Sox6 intensity (bottom) are shown underneath the figures(n=3 mice per group and 20 fields per mouse). C) *PRDM6* and *SOX6* expression level in HEK293T cells upon 22 kb CRISPR deletion of *PRDM6* intronic region. Experiments were done in triplicates. D) PRDM6 binding sites in *SOX6* gene in HEK293T cells according to ENCODE ChIP-Seq data (doi:10.17989/ENCSR892QHR). Two binding loci are zoomed for clarity E) Immunofluorescent images of *Prdm6fl/+, Prdm6fl/fl Sm22-Cre, Sox6fl/fl Sm22-Cre* and *Prdm6fl/fl Sox6fl/fl Sm22-Cre* embryonic kidneys at E18.5 labeled with SMA (red) and Renin (green) along with nuclear stain (blue). n=3 mice per group and 10 fields per genotype. The plot on the right shows the quantification of a number of cells producing Renin in four genotypes. Scale bars indicate 20 μm. IF figures: Kruskal-Wallis One-way ANOVA, **** specifies $p<0.0001$, *** $p<0.001$, * $p<0.05$. RT-qPCRs: Multiple unpaired t-tests, 2-sided. **** specifies $p<0.0001$, *** $p<0.001$, * $p<0.05$.
Note: The *Prdm6fl/+*and *Prdm6fl/fl Sm22-Cre* in Fig. 6F are shown again in 7E for comparison.

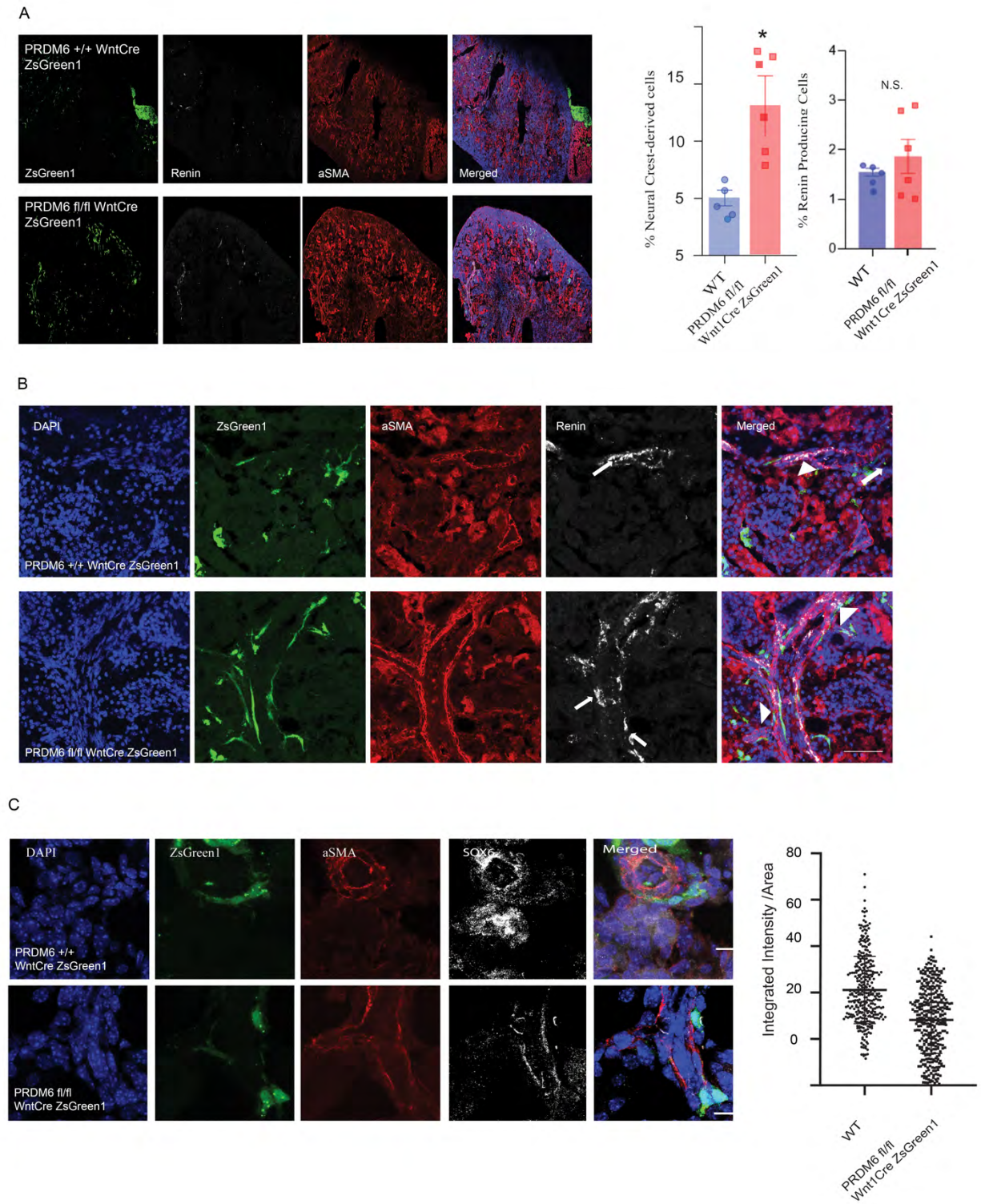

Figure 9. A) Zs1Green and renin-expressing cells in the kidneys of *Prdm6$^{fl/fl}$ Wnt1-Cre* and wild-type littermates. The plot on the right shows the quantification of Zs1Green (NCC) and renin-positive cells B) Augmented part of figure A demonstrates the close proximity of Zs1Green and renin-expressing cells on the vascular wall of in *Prdm6$^{fl/fl}$ Wnt1-Cre* kidneys marked by arrowheads. Arrows show renin. C) The localization of Sox6 in relationship to αSMA

and Zs1Greenpositive cells (NCC) in *Prdm6*$^{fl/fl}$ *Wnt1-Cre* kidneys and wild-type littermates. Scale bars indicate 20 μm. Unpaired t-test ; * $p<0.05$. n=6 mice per group in A, B and C

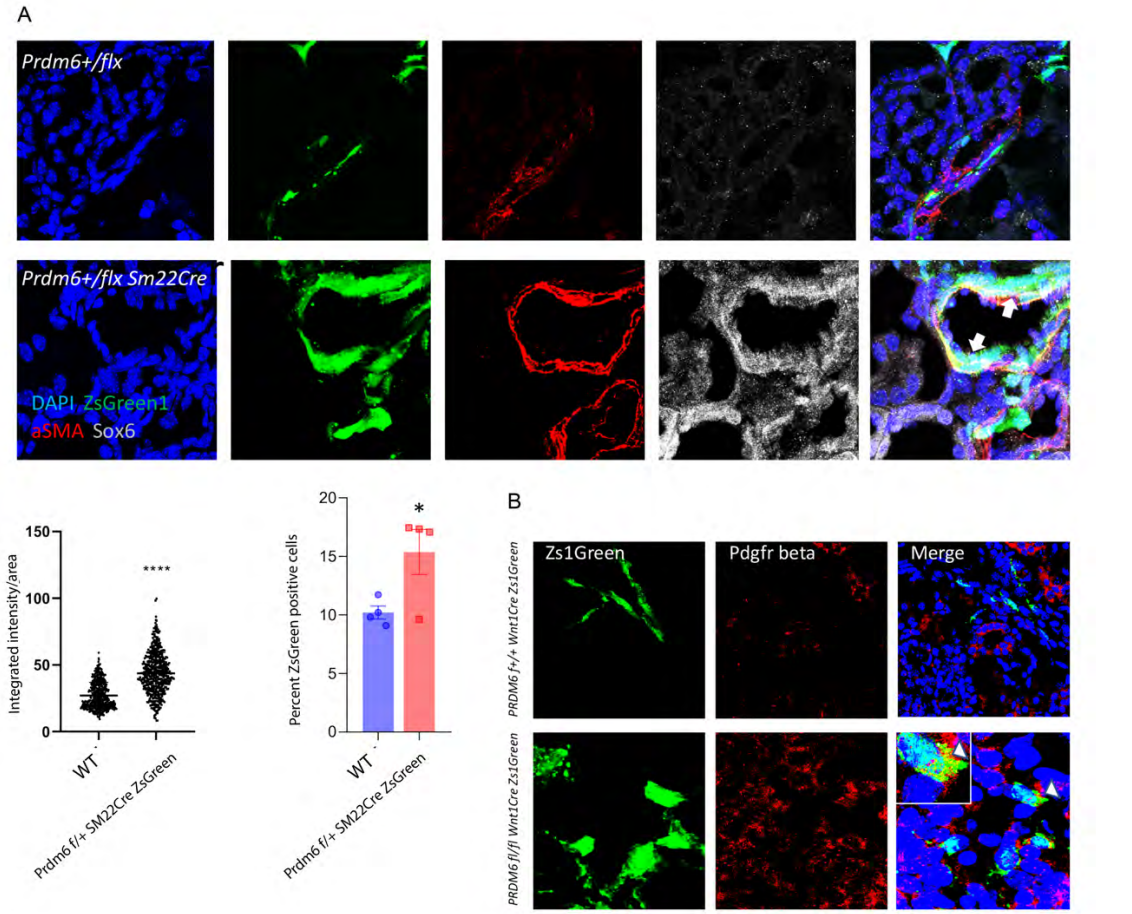
A
Prdm6+/flx
Prdm6+/flx Sm22Cre
DAPI ZsGreen1
aSMA Sox6
Integrated intensity/area
****
WT
Prdm6 f/+ SM22Cre ZsGreen
Percent ZsGreen positive cells
*
WT
Prdm6 f/+ SM22Cre ZsGreen
B
Zs1Green
Pdgfr beta
Merge
PRDM6 f+/+ Wnt1Cre Zs1Green
PRDM6 fl/fl Wnt1Cre Zs1Green
C
Prdm6 f/+
Prdm6 f/+Sm22Cre
Sirius Red
PAS
H&E
D
***
Sirius red positive area (%)
Prdm6 fl/+
Prdm6 fl/+ sm22Cre
*
Tubular diameter (μm)
Prdm6 fl/+
Prdm6 fl/+ sm22Cre
**
Glomerular diameter (μm)
Prdm6 fl/+
Prdm6 fl/+ sm22Cre
E
*
Plasma creatinine (mg/dL)
Prdm6 fl/+
Prdm6 fl/+ Sm22 Cre
ns
Plasma creatinine (mg/dL)
Prdm6 fl/+
Prdm6 fl/+ Sm22 Cre

Figure 10. A) Fate mapping of SMCs in *Prdm6fl/fl Sm22-Cre* and wild-type littermates by cross-breeding with *Zs1Greenfl/fl* mice. A) Colocalization of Sox6 and Zs1Green positive cells is shown; The integrated ZsGreen intensity per area and percent ZsGreen quantification of Sox6 in Zs1Green positive cells is compared between *Prdm6fl/fl Sm22-Cre* and wild-type littermates. n=500 cells per genotype. B) Colocalization between PDGFRβ and Zs1Green. n=4 mice per genotype C) Sirius red, PAS, and H&E staining in 12 weeks adult heterozygous *Prdm6fl/+ SM22-Cre* mice kidneys compared to wild-type mice, n=4 per group D) Tubular and glomerular diameters in *Prdm6fl/fl SM22-Cre* mice vs. wild-type littermates n=6-100 measurements. E) creatinine levels in *Prdm6fl/fl SM22-Cre* mice vs. wild-type littermates on chow and a high salt diet, respectively(Figure 9 D Scale bars indicate 20 μm. Unpaired t-test; **** specifies $p<0.0001$, **$p<0.01$, * $p<0.05$. n=5 mice per group.